

REPORT DOCUMENTATION PAGE			Form Approved OMB NO. 0704-0188	
Public reporting burden for this collection of information is estimated to average 1 hour per response, including the time for reviewing instructions, searching existing data sources, gathering and maintaining the data needed, and completing and reviewing the collection of information. Send comment regarding this burden estimate or any other aspect of this collection of information, including suggestions for reducing this burden, to Washington Headquarters Services, Directorate for Information Operations and Reports, 1215 Jefferson Davis Highway, Suite 1204, Arlington, VA 22202-4302, and to the Office of Management and Budget, Paperwork Reduction Project (0704-0188), Washington, DC 20503.				
1. AGENCY USE ONLY (Leave blank)	2. REPORT DATE September 10, 1996	3. REPORT TYPE AND DATES COVERED Final 15 Jul 94 - 14 Jul 95		
4. TITLE AND SUBTITLE Instrumentation for Investigating Precursors to High Reynolds Number Unsteady Flow Separation on Pitching Airfoils		5. FUNDING NUMBERS DAAH04-94-G-0268		
6. AUTHOR(S) Sumon K. Sinha, Dipankar Pal, Debjyoti Banerjee, Mukesh Pandey, and Chuck Baker				
7. PERFORMING ORGANIZATION NAME(S) AND ADDRESS(ES) The University of Mississippi Old Chemistry Building University, MS 38677		8. PERFORMING ORGANIZATION REPORT NUMBER ARO/FRI/996		
9. SPONSORING / MONITORING AGENCY NAME(S) AND ADDRESS(ES) U.S. Army Research Office P.O. Box 12211 Research Triangle Park, NC 27709-2211		10. SPONSORING / MONITORING AGENCY REPORT NUMBER ARO 33154.1-EG-DPS		
11. SUPPLEMENTARY NOTES The views, opinions and/or findings contained in this report are those of the author(s) and should not be construed as an official Department of the Army position, policy or decision, unless so designated by other documentation.				
12a. DISTRIBUTION / AVAILABILITY STATEMENT Approved for public release; distribution unlimited.		12 b. DISTRIBUTION CODE 19961023 247		
13. ABSTRACT (Maximum 200 words) A pitching airfoil test facility has been developed to enable investigating the unsteady flow separation process on helicopter rotor blades under flow conditions which replicate the viscous-inviscid interactions. The facility is capable of operating at chord based Reynolds numbers of 10^6 and reduced frequencies of 0.23 while maintaining the Mach number below 0.15. A multi-element compliant wall sensor has been developed to measure pressure fluctuations just preceding the eruption of the boundary layer. Following successful implementation on cylinders and non-pitching airfoils, this transducer has been used to detect the propagation of wall pressure fluctuations in the neighborhood of the separation point. Preliminary data obtained by sampling simultaneously the data from eight transducer strips has revealed patterns characteristic to the boundary layer eruption process.				
14. SUBJECT TERMS Unsteady Flow Separation, Dynamic Stall		15. NUMBER OF PAGES 47		
		16. PRICE CODE		
17. SECURITY CLASSIFICATION OF REPORT UNCLASSIFIED	18. SECURITY CLASSIFICATION OF THIS PAGE UNCLASSIFIED	19. SECURITY CLASSIFICATION OF ABSTRACT UNCLASSIFIED	20. LIMITATION OF ABSTRACT UL	

DISCLAIMER NOTICE



**THIS DOCUMENT IS BEST
QUALITY AVAILABLE. THE
COPY FURNISHED TO DTIC
CONTAINED A SIGNIFICANT
NUMBER OF PAGES WHICH DO
NOT REPRODUCE LEGIBLY.**

SUPPLEMENTARY

INFORMATION

November 20, 1996

ERRATA
ADA 316875

Delores

Per our telephone conversation this date I'm sending the following:

A Final Report was sent to DTIC last month with the SF 298 in **block 5** as grant

DAAH04-94-G-0268 and **block 10** as ARO 33154.1-EG-DPS

PLEASE MAKE THE ABOVE TO READ:

SF298 Block 5 DAAH04-93-G-0451

SF298 Block 10 ARO 32404.1-EG-DPS

Also the change needs to be made on the DTIC form 50 card, so when it is returned to me I will credit the final report to ARO 32404.1-EG-DPS, grant number DAAH04-93-G-0451.

ERRATA

Thank you,

Sylvia, ICA
Army Research Office

ADA 316875

INSTRUMENTATION FOR INVESTIGATING PRECURSORS TO HIGH REYNOLDS
NUMBER UNSTEADY FLOW SEPARATION OVER PITCHING AIRFOILS

FINAL PROGRESS REPORT

BY
SUMON K. SINHA, DIPANKAR PAL, DEBJYOTI BANERJEE, MUKESH PANDEY AND
CHUCK BAKER

SEPTEMBER 10, 1996

U.S. ARMY RESEARCH OFFICE

GRANT NUMBER: DAAH 04-93-G-0451

THE UNIVERSITY OF MISSISSIPPI

APPROVED FOR PUBLIC RELEASE;

DISTRIBUTION UNLIMITED.

THE VIEWS OPINIONS, AND/OR FINDINGS CONTAINED IN THIS REPORT ARE THOSE
OF THE AUTHORS AND SHOULD NOT BE CONSTRUED AS AN OFFICIAL DEPARTMENT
OF THE ARMY POSITION, POLICY, OR DECISION, UNLESS SO DESIGNATED BY OTHER
DOCUMENTATION.

TABLE OF CONTENTS

1.	Table of Contents	1
2.	I. Introduction	2
	II. Facilities and Instrumentation Developed	2
	a) Flow Facility Upgrade	2
	b) Instrumentation	3
	III. Results	4
	IV. Project Personnel	4
	V. Publications Attributable to the Project	5
3.	References	5
4.	Figures	
	Figure 1. Schematic of recirculating wind tunnel	6
	Figure 2. Photograph of test section	7
	Figure 3. Acoustosurf Cross Section	8
	Figure 4. NACA-0012 airfoil with strips	8
	Figure 5. Photographs of cylinder flow	9
	Figure 6. Spectra of signals from static airfoil case	10
	Figure 7. Effect of excitation	10
	Figure 8. Pitching airfoil data from eight strips	11
5.	Appendix (Includes copies of 3 papers and 1 M.S. Thesis Abstract Resulting from this grant)	12

Introduction

Many of the important features of the flow over a helicopter rotor blade can be reproduced in the nominally two-dimensional flow over a pitching airfoil. One such feature is a dynamic stall, which is initiated by unsteady flow separation on the suction side of the blade. A full-blown dynamic stall causes an extremely large and rapid increase in flow induced pitching moments. This can lead to premature mechanical failure. Although, this situation is avoidable during normal operations, it is inevitable during high speed evasive combat maneuvers. Therefore, methods for detecting an oncoming flow separation and preventing it from developing into a full-blown stall is of particular interest. The present work is an attempt to identify precursors to unsteady flow separation on pitching airfoils by measuring flow-induced surface pressure fluctuations in the vicinity of the separation point. These precursors can then be used to direct a small control input, such as boundary layer suction, to delay or prevent the progression of the oncoming stall.

As a result of previous studies (both experimental and computational), many of the characteristic features of the above mentioned unsteady separation have been reasonably well understood and documented for low Reynolds numbers (i.e., Re values typically less than 500,000 based on the chord). Typically, flow separation commences when the boundary layer erupts and vorticity is ejected into the inviscid freestream. The eruption process is initiated over a very small portion of the suction surface. As per the approaches of Elliott et. al. (1983) and Smith (1986), the streamwise extent of the eruption can be scaled as $Re^{-5/11}$ of the airfoil chord. Re values of prototype blades generally exceed 2×10^6 , and the flow separation characteristics of airfoils have been observed to undergo changes around Re values of 5×10^5 (Abbott and von Doenhoff, 1959), primarily due to a pre-separation laminar-turbulent transition. Hence, a specific need exists to identify flow separation precursors under these conditions. The work described here relates to the development of facilities and instrumentation for this study. The approach taken aims at measuring wall pressure fluctuations (e.g., Farabee and Casarella, 1988; and Simpson et al., 1987) with adequate spatial and temporal resolution in the vicinity of the separation point.

Facilities and Instrumentation Developed

Flow Facility Upgrade: The studies were based primarily on an existing recirculating wind tunnel at the University of Mississippi as shown in Figure 1. Funds from this grant were utilized to improve the flow characteristics of the tunnel. This included introducing a honeycomb flow straightener in place of existing window-screens at the entrance to the contraction section. This reduced the large scale unsteadiness present in the tunnel, resulting in a highest mean velocity of about 50 m/s in the 600-mm x 420-mm test section. The freestream turbulence level at the highest speed was just under 1%. A new test section was designed and fabricated (Figure 2) to incorporate a 300-mm chord, 420-mm span oscillating wing model. Thus, with the present setup it is possible to reach Re values of about 10^6 and reduced frequencies of about 0.23. The maximum freestream Mach number was about 0.15.

The test section utilized a variable speed D.C. motor with a speed controller driving the oscillating airfoil through a four-bar crank mechanism. The airfoil models used were based on a Styrofoam core with a 1/16-inch thick balsa-wood skin epoxied on. This technique enabled fabricating light-weight and rigid wing sections. The wing sections were supported at both tips.

Each tip was fastened to an oscillating 280-mm diameter clear acrylic window, so as to permit flow visualization while oscillating the wing about its 1/4-chord axis. The wing sections could be easily instrumented with microphones or other wall mounted or flush mounted sensors.

The setup for flow visualization included acquiring a theatrical fog generator so as to introduce sufficient quantities of non-toxic smoke into the test section. The smoke was introduced through a streamlined rake located just downstream of the flow straighteners. A 5-Watt Argon-ion laser and optical hardware (including lenses and a fiber-optic light-sheet probe) was acquired to illuminate the plane of the smoke rake. Finally, an arrangement for venting the air in the test section was developed so as to periodically clear the smoke.

Instrumentation: The oscillating test section was mechanically coupled to an optical incremental angular position encoder acquired for this purpose. The encoder output was used to trigger the data acquisition sequence as described in the following sections. A pulse counting circuit was used for setting the trigger position at any location in 0.1-degree increments. A 486-based microcomputer system was purchased for acquiring pressure fluctuation data close to the stall point of the oscillating airfoil. Eight 8-bit 20-MHZ A/D data acquisition boards were installed along with the requisite software to permit acquiring data from eight spatially distributed sensors simultaneously. In this manner the spatial and temporal development of wall pressure fluctuations could be recorded without suffering loss in information due to multiplexing. Other data, such as mean pressures, sound pressure levels and velocity components were also measured.

Recent studies by Dr. Sinha's research group resulted in the development of an active compliant wall transducer, the "Acoustosurf" (Sinha, 1996; Sinha and Pal, 1994; and Sinha et al. 1996) for flow separation control. This transducer consists of an array of electrostatically activated conducting strips driving a flexible surface as shown in Figure 3. A small amount of air is trapped between the surface of each strip and the outer flexible sheet. A D.C. bias voltage is applied to each strip. When the outer flexible surface is exposed to a flow, it responds primarily to the flow-induced wall pressure fluctuations. The outer flexible surface can also be driven electrically. Thus, the same transducer can be used both as a sensor as well as an actuator. Initial experiments by Sinha and Pal (1994) indicated the presence of a characteristic frequency for unsteady separating flows over cylinders, as sensed by one of the transducer strips. Electrical excitation at this frequency resulted in a downstream movement of the separation point and suppression of vortex shedding.

For the present study, the transducer was mounted near the leading edge of the test NACA-0012 wing section as shown in Figure 4. For the pitching airfoil studies eight 1-mm wide strips with 1-mm gaps were used. In order to make the strips truly independent of each other electrically, each strip was individually biased using a bank of gel cells. The gel cells also greatly reduced the electrical noise in the signal compared to using a line-driven D.C. power supply.

A major challenge in this investigation was the accurate detection of the separation point. Flow visualization could be used to locate the point within ± 1 -mm. However, for the Reynolds numbers in question, the boundary layer eruption process can be expected to occur over a streamwise length scale of about 0.5-mm or less. It is convenient to have an array of strips close to this point. If the flow parameters (Re and reduced frequency) change, it is not necessary to physically move the transducers to track the separation point. This is why the original proposed approach of using an array of miniature microphones mounted under the surface was not followed. However, the miniature microphones were acquired so as to compare results for some selected cases.

Results

The grant in question was used to acquire the instrumentation and set up the facilities as described above. The research is currently in progress and is being supported by ARO through Grant No. DAAH 04-94-G-0268. In this section some preliminary results are described which demonstrate the feasibility of the experimental approach.

The use of the multi-strip transducer in detecting characteristic fluctuation frequencies in separating boundary layers was first demonstrated on the unsteady separating boundary layer on a cylinder. A transducer strip located 72° from the leading edge of a cylinder detected a characteristic frequency of 2.25 kHz for a diameter based Reynolds number of 1.5×10^5 . Exciting the strips located between 72 - 78° resulted in moving the separation point from about 78° to 106° in this marginally subcritical flow. The flow visualization system incorporated in this project was used to verify the control as shown in Figure 5.

Following the cylinder experiments, the process was repeated on an NACA 0012 airfoil under static stall conditions. The airfoil was set at an angle where the flow just separated for the Reynolds number in question. Signals from single strips revealed several characteristic peaks in their frequency spectra (Figure 6). Exciting the same strips electrically resulted in changing the velocities in the wake as sensed by a hot-film sensor (Figure 7). Maximum changes were observed at two frequencies: 2-kHz and 4.5 kHz at a chord based Re of 4.3×10^5 as seen in Figure 7. Flow visualization revealed that partial reattachment of the separated boundary layer occurred at 2-kHz, while a complete reattachment occurred at 4.5 kHz. Since these studies were done before the honeycomb flow straighteners were installed, the quality of the resulting flow visualization photographs was poor. Hence, these have not been shown here. These studies also resulted in redesigning the transducer for higher Reynolds numbers.

For the preliminary pitching airfoil studies, signals from eight consecutive strips near the leading edge of the NACA-0012 were acquired every $0.1 \mu\text{s}$ over a 0.8 ms interval, near the beginning of the flow separation process. For $\text{Re} = 10^6$ and $k = 0.23$ a typical data set is shown in Figure 8. The data acquisition boards were triggered at an angle of attack of 22° while the airfoil was oscillated between 5° and 25° at 6.7 Hz. Flow visualization revealed that the flow separation commenced around 22° for this case. Figure 8 indicates that the level of pressure fluctuations sensed by channel-4A (the seventh strip from the leading edge) is significantly lower than strips upstream and downstream. Additionally, channels 1A-3B indicate a downstream moving wave-like disturbance. From this data it may seem that the boundary layer begins erupting over the seventh strip. However, this is yet to be confirmed by the ongoing experiments.

Project Personnel

Principal Investigator: Dr. Sumon K. Sinha

Graduate Students: Dipankar Pal (Ph.D.)
 Debjoyoti Banerjee (M.S.) (Completed M.S. with support from project)
 Mukesh Pandey (M.S.)

Undergraduate Students:

Chuck Baker (played a key role in setting up the data acquisition system and processing preliminary data)

Randel Harbur, Henry Lee Jones and Clark Love (design and fabrication of the pitching mechanism and safety enclosure for the facility)

Publications attributable to the project

1. Sinha, S.K., Pal, D., and Banerjee, D., "Control of Flow Separation using the EMEMS Approach: Proof of Concept Experiments," International Mechanical Engineering Congress and Exposition, Microfluids Symposium, Atlanta, Nov 17-22, 1996 (Accepted after review of manuscript; to be presented and published in the symposium bound volume. Preprint attached).
2. Pal, D., Sinha, S.K., Banerjee, D., Baker, C., and Pandey, M., "A Compliant Wall Sensor Array for Detecting Pressure Fluctuation Signatures in Separating Boundary Layers," AIAA Paper No. 97-0391, AIAA Aerospace Sciences Meeting, Reno, Jan 1997 (Accepted based on initial draft, final version under preparation. Initial draft attached).
3. Pal, D., and Sinha, S.K., "Controlling an Unsteady Separating Boundary Layer on a Cylinder with an Active Compliant Wall," AIAA Paper No. 97-0212, AIAA Aerospace Sciences Meeting, Reno, Jan 1997 (Accepted based on initial draft, final version under preparation. Initial draft attached).
4. Banerjee, D., "An Experimental Investigation of Flow Separation Control using an Acoustic Active Surface", M.S. Thesis, University of Mississippi, 1995. (Abstract attached)

References

1. Abbott, I.H., and von Doenhoff, A.E., Theory of Wing Sections, Dover Publications, 1959.
2. Elliott, J.W., Smith, F.T., and Cowley, S.J., "Breakdown of Boundary Layers: I) On Moving Surfaces; ii) In Semi-Similar Unsteady Flow; iii) In Fully Unsteady Flow," Geophys. Astrophys. Fluid Dynamics, 1983, Vol.25, pp. 77-138.
3. Farabee, T.M., and Casarella, M.J., "Wall Pressure Fluctuations beneath a Disturbed Turbulent Boundary Layer", International Symposium on Flow Induced Vibration and Noise", 1988, Vol.6, pp. 121-135.
4. Simpson, R.L., Ghodbane, M., and McGrath, B.E., "Surface Pressure Fluctuations in a Separating Turbulent Boundary Layer", Journal of Fluid Mechanics, Vol. 177, 1987, pp. 167-186.
5. Sinha, S.K., "The ACOUSTOSURF - a Multi-Element Acoustic Active Surface for Flow Separation Control", 1996 Patent pending.
6. Sinha, S.K., and Pal, D., "Controlling Unsteady Separation with Acoustic Active Surfaces", 1994, AIAA Paper No. 94-0183.
7. Sinha, S.K., Pal, D., and Banerjee, D., "Control of Flow Separation using the EMEMS Approach: Proof of Concept Experiments," International Mechanical Engineering Congress and Exposition, Microfluids Symposium, Atlanta, Nov 17-22, 1996.
8. Smith, F.T., "Steady and Unsteady Boundary-Layer Separation", Annual Review of Fluid mechanics, Vol. 18, 1986, pp. 197-220.

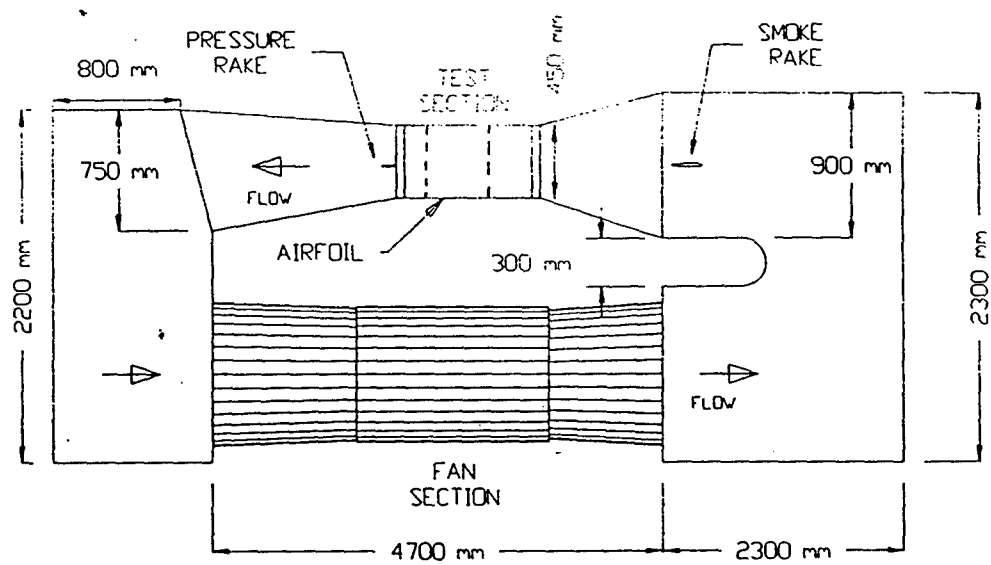


Figure 1. : Schematic of recirculating wind tunnel .

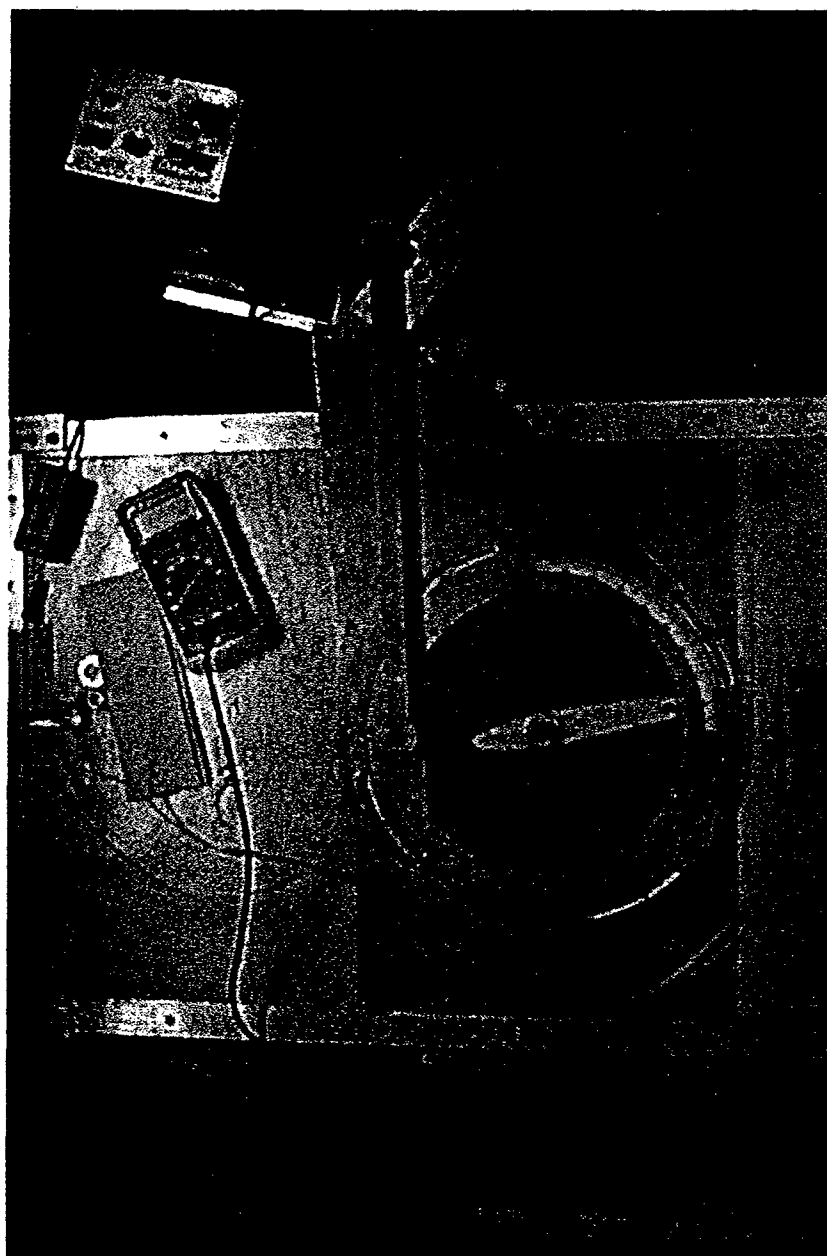


Figure 2. : Photograph of test section .

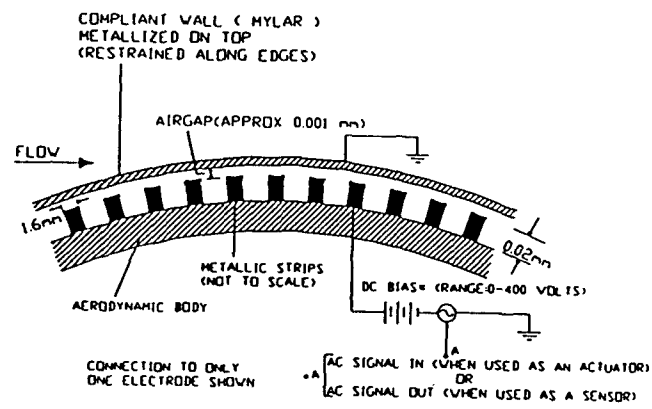


Figure 3. : Acoustosurf Cross-section

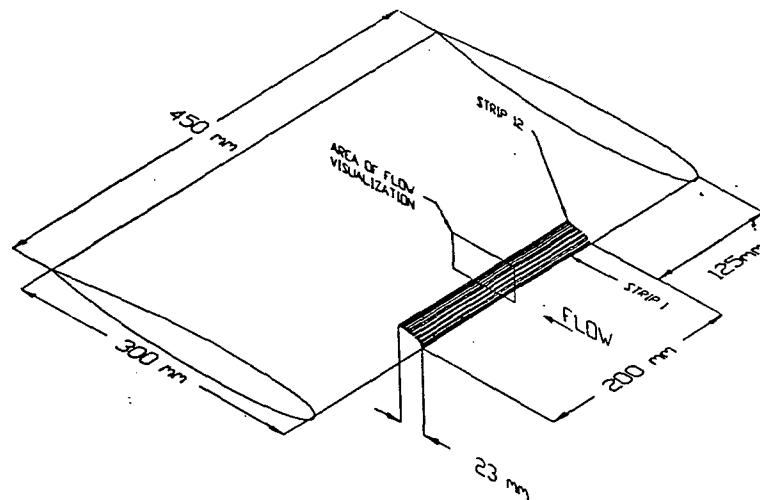


Figure 4. : NACA0012 airfoil with strips

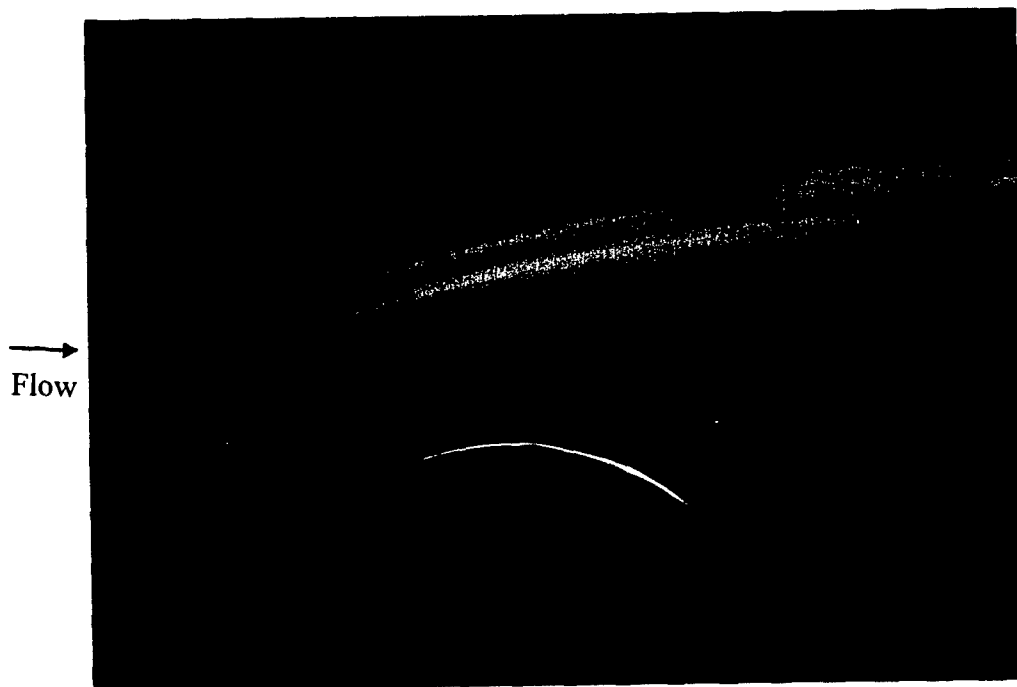


Figure 5.(a) : Photograph of cylinder flow (Untripped case)

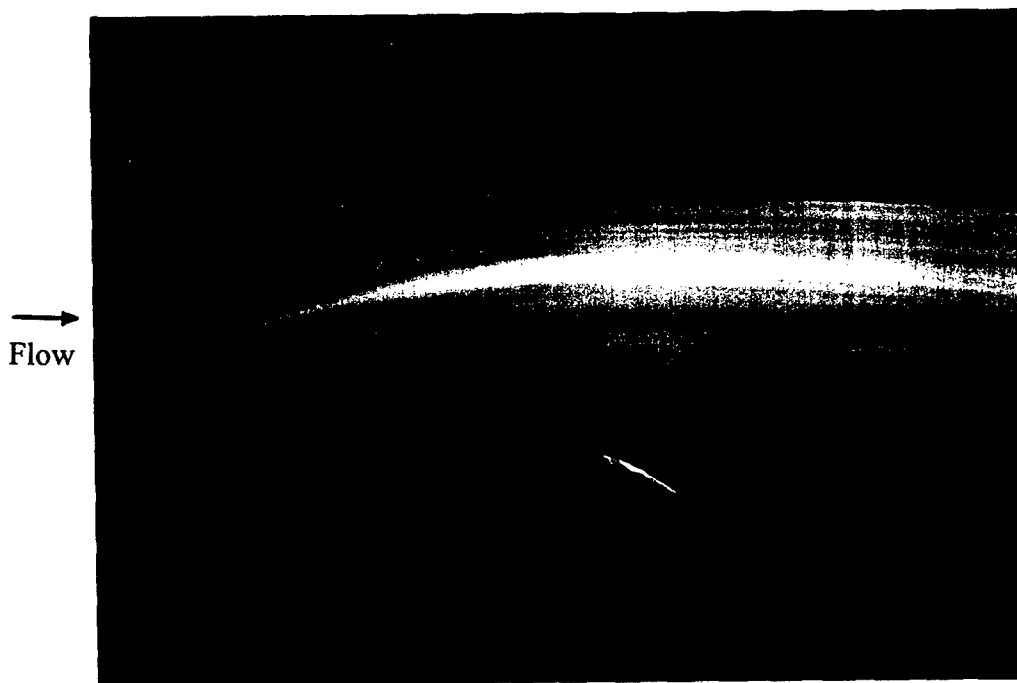


Figure 5.(b) : Photograph of cylinder flow (Tripped case)

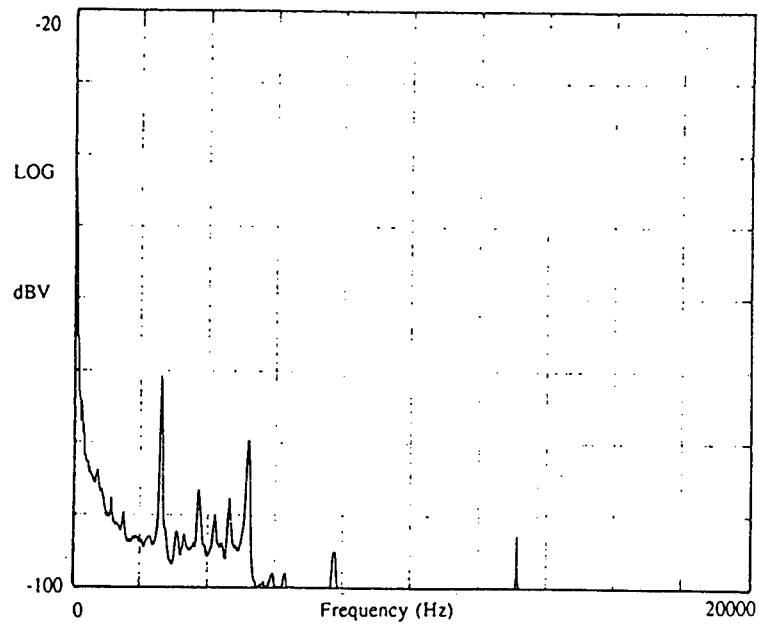


Figure 6. : Spectra of signals from static airfoil case.

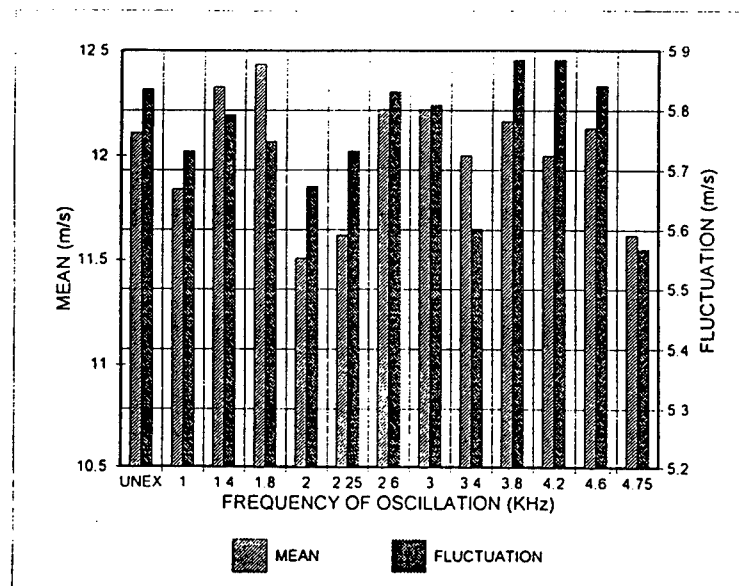


Figure 7. : Effect of excitation.

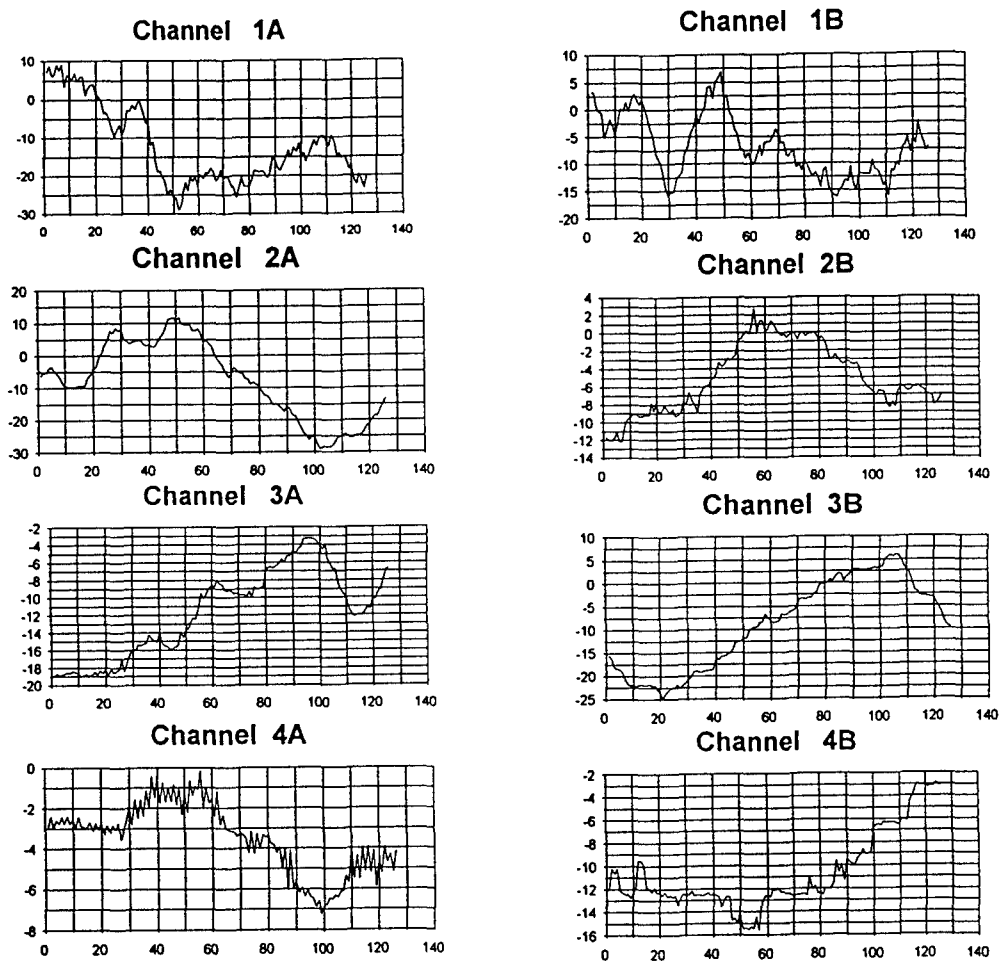


Figure 8. : Pitching airfoil data from eight strips.

Appendix

Copies of the following publications attributable to the project are attached in the following order:

1. Sinha, S.K., Pal, D., and Banerjee, D., "Control of Flow Separation using the EMEMS Approach: Proof of Concept Experiments," International Mechanical Engineering Congress and Exposition, Microfluids Symposium, Atlanta, Nov 17-22, 1996.
2. Pal, D., Sinha, S.K., Banerjee, D., Baker, C., and Pandey, M., "A Compliant Wall Sensor Array for Detecting Pressure Fluctuation Signatures in Separating Boundar Layers," AIAA Paper No. 97-0391, AIAA Aerospace Sciences Meeting, Reno, Jan 1997.
3. Pal, D., and Sinha, S.K., "Controlling an Unsteady Separating Boundary Layer on a Cylinder with an Active Compliant Wall," AIAA Paper No. 97-0212, AIAA Aerospace Sciences Meeting, Reno, Jan 1997.
4. Banerjee, D., "An Experimental Investigation of Flow Separation Control using an Acoustic Active Surface", M.S. Thesis, University of Mississippi, 1995. (Abstract attached)

CONTROL OF FLOW SEPARATION USING THE EMEMS APPROACH: PROOF OF CONCEPT EXPERIMENTS

Sumon K. Sinha, Dipankar Pal and Debjyoti Banerjee*

Mechanical Engineering Department

University of Mississippi

University, MS 38677

Phone: 601-232-5374, FAX: 601-232-7219,

email: mesinha@olemiss.edu

ABSTRACT

A driven flexible wall transducer has been developed for controlling unsteady and steady separating flows. The transducer consists of an array of electrostatically active strips under a flexible surface. The transducer is at first used as a sensor to detect wall pressure fluctuation frequencies which are believed to correspond to instabilities in the attached boundary layer and the separated shear layer. Next, selected transducer strips are driven at one of the sensed frequencies so as to introduce vortices close to the wall. Reattachment can occur when these vortices move downstream to the separated shear layer. This method has been used to control transcritical flow separation on a circular cylinder (Re of 1.5×10^5) and reattach marginally separated boundary layers on an NACA 0012 airfoil at Re values slightly under 10^6 . To increase the strength and reduce the size of the controlling vortices, an elastomeric microstructured (EMEMS) version of this transducer is presented. The EMEMS transducer also has the potential of being robust and inexpensive.

INTRODUCTION

Controlling boundary layer flow separation is of interest for a variety of practical engineering problems. The onset of flow separation usually limits the maximum performance attainable by devices employing lifting surfaces. Methods aimed at delaying or preventing separation have the potential of extending the operational regime of such devices. Examples of such devices range from aircraft wings to compressor blades and pump impellers. In order to prevent or delay flow separation, the velocity profile in the boundary layer has to be modified. Traditionally, this is achieved either by removing the low-momentum fluid or by re-energizing the slow wall-layer by injecting high-momentum fluid or enhancing mixing in the boundary layer.

The design and selection of a device for flow separation control is primarily based upon the efficacy of the device in providing

the control. Other considerations include, the degree of interference with the flow when no control is needed, and compatibility of the device with the operating environment. In order to satisfy these conditions, several non-traditional techniques for controlling separation have emerged (Gadel-Hak and Bushnell, 1991). In spite of these advances, the implementation of effective flow separation control remains a challenge on high-speed rotating lifting-surfaces. Rotating stall on axial compressor blades and dynamic stall on helicopter rotors are examples of undesirable flow separation induced effects involving rotating lifting-surfaces. Boundary layer flow separation on such surfaces is usually unsteady, since the spatial location of the separation point and the instant of time when the flow separates are generally not known a priori. Additionally, the high-stress mechanical environment severely limits the choice of hardware. The present work was initiated in order to develop a practical device for such situations. The final design developed is based on an elastomeric microstructured electro-mechanical system or EMEMS. The rationale leading to this design, including proof of concept experiments, are described in this paper.

WHY USE MEMS FOR FLOW SEPARATION CONTROL

Passive devices, such as wall mounted vortex generators, generally contribute towards an unacceptably large drag penalty when used to control unsteady and intermittently separating flows. For optimum control of unsteady separation, an array of sensors is needed to direct the appropriate control input from an array of actuators to the correct location at the right instant in time. To accomplish this effectively, without introducing an unacceptable level of mechanical complexity, an array of small scale sensors and actuators as afforded by MEMS is seen as the best solution.

MEMS based devices can be expected to manipulate small-scale flow features in a boundary layer. These have to eventually control flow separation, which is a large-scale feature. Hence, the relationship between small scale perturbations and large scale features has to be

*Present Affiliation: MAE Dept., Univ. of California-Los Angeles
Los Angeles, CA 90024

exploited, such that low energy control perturbations can be used to modify a large energy mean flow. This can be achieved by exploiting non-linearities and instabilities inherent in the flow and applying a small control input only where and when it is needed, making this approach inherently energy efficient. The second advantage is that control devices and strategies at the small scale may not be as application specific as their large scale counterparts.

WHY DEVELOP THE EMEMS TRANSDUCER

McMichael (1996) has recently reviewed MEMS based active devices and strategies for flow control. The general focus of the research community has been to develop MEMS primarily for reduction of skin friction in boundary layer flows. Additionally, in order to make effective use of existing silicon-based electronic microfabrication technology, most MEMS devices currently being investigated are silicon based. Successful examples of silicon based boundary layer flow control devices include, microflaps (Tsao et al., 1994) and micron scale floating element shear stress gages (Padmanabhan et al., 1995). However, silicon is brittle and it cannot withstand large elastic strains. This has often forced MEMS designers to use mechanical motion amplifiers, such as bending beams. This unfortunately complicates the designs of MEMS transducers and contributes towards increasing their cost per unit area.

To further MEMS technology for flow control, simpler forms of transducers need to be developed which do not suffer from the shortcomings outlined above and are capable of controlling high-Reynolds number unsteady separating flows. Within these constraints, possibilities include driven flexible walls, a wall with active blowing suction ports or a wall with imbedded heating/cooling elements. All of these devices have been known to interact with and modify boundary layer flows (e.g., see review article by Gad-el-Hak and Bushnell, 1991).

In the present case, the intended applications were to gas flows on rotating lifting surfaces. Furthermore, designs were restricted to devices requiring minimum sub-surface machining of the flow surface. This effectively eliminated wall blowing and suction. Thermal transducers could be considered, as long as they did not have to cool the boundary layer, since heat removal necessitates the use of imbedded sub-surface heat sinks or heat pipes. However, cooling is needed to reduce the viscosity close to the wall in gas flow boundary layers. Reducing the viscosity near the wall increases the near wall momentum, thereby helping delay flow separation. Heating the wall has the opposite effect. Therefore, thermal transducers were eliminated from further consideration and the internally driven flexible wall was judged as the most viable option. Driving the transducer surface through mechanical power transmission elements like levers, or shafts, was ruled out. The internal driving was to be achieved by using an array of acoustic transducers, since acoustic speakers or microphones based on electromagnetic, electrostatic or piezo-electric forcing are inherently simple and robust.

To retain the mechanical simplicity of the design, it was decided that the acoustic driving elements of the transducer would also have to serve as sensors (Bandyopadhyay, 1995). To achieve this, the flexible surface had to be mounted on a compliant substrate. This arrangement can enable direct sensing of flow induced wall vibrations. The dynamic response of the sensor array can be customized by selecting a substrate material having the requisite elastic and dissipative properties. If an elastomeric substrate is used, with the spacing and size of the transducer elements miniaturized, the final result is an "Elastomeric

Micro-fabricated Electro-Mechanical System" or EMEMS.

SEPARATION CONTROL USING ACTIVE AND PASSIVE COMPLIANT WALLS

Ever since the pioneering work of Kramer (1960) on the role of compliant wall coatings in inhibiting flow induced surface wave growth, a large number of experimental, theoretical and computational studies have been undertaken in this area. The broad emphasis of these studies has been towards achieving reduction of skin-friction drag by either delaying transition to turbulence or by manipulating the bursting events in a turbulent boundary layer (Gad-el-Hak, 1989, 1994). However, methods to alter skin friction can also be used to delay or promote flow separation and will be briefly reviewed here.

Early experiments by Wehrmann (1965) showed that a driven flexible wall could be used to control the onset of flow transition by enhancing or attenuating Tollmien-Schlichting instability waves. Bushnell et al. (1977) concluded that passive compliant walls are incapable of producing short wavelengths along with moderate oscillation amplitudes believed to be necessary for reducing skin friction in turbulent air boundary layers. Subsequent studies by Weinstein (1981), using an acoustic horn driven flexible wall transducer, have shown that moderate amplitude (around 0.1 mm) wall oscillations in the frequency range of 0.5 to 2.2 kHz could not modify the mean velocity profile appreciably in a tripped boundary layer on a flat plate. This work also showed that acoustic radiation from the surface had only small effects on the Reynolds stress components.

A review of literature failed to reveal any previous investigations which have explicitly stated the use of compliant walls for separation control. However, the effect of vibrations on flow separation can be observed in experiments with acoustic sources (e.g. Ahuja and Burrin, 1984; and Zaman, 1992). Although, the original investigators attributed their observations to acoustic radiation, subsequent studies have shown that non-acoustic effects associated with these sources usually play the dominant role. For example, this is seen in the flow separation control experiments of Williams et al., (1991) and Sinha and Pal (1993), where a sound source mounted inside the model was used to perturb the boundary layer through a slot. The main effect was due to the alternate blowing and suction at the slot and not the emitted acoustic radiation.

The effective frequencies were found to increase with the flow Reynolds number. Although, acoustic speakers can produce large sound pressure levels at higher frequencies, the efficacy of the control was found to reduce with increasing Re. The acoustic speaker induced blowing/suction effect needed more power as the flow Reynolds number increased. Therefore, it was believed that a transducer which directly introduced the velocity fluctuations at the surface would be more effective. This resulted in the development of an active driven wall transducer described below.

THE "ACOUSTOSURF": AN ACTIVE COMPLIANT WALL TRANSDUCER FOR FLOW SEPARATION CONTROL

The first transducer which was developed, based on the considerations outlined in the previous section, was the "Acoustosurf" (Sinha, 1996). The Acoustosurf consists of a thin flexible dielectric (Mylar) sheet with its outer surface made electrically conductive by depositing aluminum (Fig. 1). This sheet (to be referred to henceforth as

the outer sheet) is stretched across an array of thin and nearly flush-mounted conducting strips (referred to as the substrate). The strips may be individually glued to the surfaces or be formed by etching out a flexible copper clad plastic (polyamide) sheet. Both designs have been investigated and virtually no differences have been observed on their effects on flow control. If the second approach is used (the preferred approach), the Acoustosurf takes the form of a thin flexible composite sheet. The back of the etched copper clad sheet is then glued on to the aerodynamic surface (e.g., the surface of a rotor blade or wing). This forms the substrate. The outer sheet is then stretched over it and glued to the substrate around its periphery. A DC bias voltage, applied between the conducting outer surface of the outer sheet and the conducting strips, controls the tension in the flexible sheet. The bias voltage also controls the thickness of the air gap between the outer sheet and the substrate. The maximum permissible DC bias is limited primarily by the electrical breakdown voltage of the outer sheet.

When an AC voltage is superimposed on the DC bias, the portion of the outer sheet on top of a conducting strip will execute vibrations corresponding to the AC signal applied to the strip. Thus, the segment of the outer sheet above each strip can be excited nearly independently. Several strips can be actuated at different frequencies and phases, thereby permitting the generation of any desired surface oscillation pattern (including standing waves and traveling waves). The effective stiffness and damping of the vibrating outer surface can be controlled by adjusting the bias voltage. The amplitude of surface oscillation can be varied by controlling the AC voltage. The surface vibrations also result in sound radiation from the surface. Thus, the Acoustosurf can also serve as an array of acoustic sources.

Segments of the outer sheet between the conducting strips are not directly energized from below. However, these segments have a slightly larger pocket of air trapped below them. This feature allows the un-energized sections to respond to surface pressure fluctuations. This feature is described further in the next section.

Interaction with the flow

When the Acoustosurf is mounted on an aerodynamic surface, the flow of air over the surface oscillates the free segments of the outer sheet in between the conducting strips. The frequency and mode of these oscillations depend on the coupling of the flow with this compliant wall. These oscillations also induce fluctuations in the air gap between the outer sheet and the conducting strips. This results in a variation in the electrical capacitance. When a DC bias is applied, the voltage between a conducting strip and the outer sheet will fluctuate as per the sensed pressure changes. The fluctuating voltage signal can now be extracted by blocking the DC. This signal, which contains information about the flow, can be used for determining the frequency, spatial location, temporal phase and wave number for actuation so as to obtain the desired effect. It is to be noted however, that the same strip cannot be used as an actuator while it is being used as a sensor.

In the actuator mode, AC signals to the strips drive the surface through electrostatic forcing. The amplitude of oscillation is typically in the order of a few microns. Thus, the oscillations can only directly force the fluid layer very close to the wall. For most boundary layer flows such forcing is too small to produce any measurable changes. However, significant changes may be observed provided the oscillations are introduced in regions of the boundary layer where flow instabilities exist. The flow then amplifies the introduced disturbances. The Acoustosurf

can be seen to provide a means for introducing low-energy small-amplitude perturbations into a boundary layer. This occurs when the natural frequencies and modes of the flow induced surface oscillations coincide with those produced by internal electrical driving.

The amplified disturbances propagate with the flow. If the frequency of the amplified disturbances also coincides with an instability frequency of the free shear layer downstream of the point of separation, the non-linear amplification process of these instabilities is modified. This usually results in the reattachment of the separated shear layer.

Separation Control Strategy Using the Acoustosurf

The Acoustosurf apparatus described can be utilized for controlling unsteady separation on an aerodynamic surface using a sensor-actuator feedback loop configuration. The array of strips needs to span the area over which separation can occur. In the case of three-dimensional separation, each strip can be divided into smaller segments thereby creating a checkerboard pattern of transducers. Signals from the appropriate transducer elements can be acquired and analyzed to determine the spatial and temporal structure of naturally occurring flow-induced wall pressure fluctuations. This can be achieved by comparing the acquired signals to those that have been found to occur during the onset of flow separation. Once the location and time of the separation have been estimated, the appropriate transducer elements are used as actuators. Perturbations are introduced into the separating (or just separated) region of the boundary layer in order to delay the separation or reattach a separated shear layer.

Experimental Verification

The strategy described above outlines the general procedure. Some parts of this procedure have been experimentally verified as outlined here. The first set of experiments were conducted in a low-speed subsonic wind-tunnel (maximum velocity about 15 m/s). A 152-mm diameter circular cylinder was placed in crossflow in the tunnel test section. A section of the Acoustosurf, with 1.6-mm wide strips, with 1.6-mm spacing, was mounted on the top surface of the cylinder. The strips were oriented parallel to the cylinder axis. Best results were obtained at a diameter based Reynolds number (Re) of 1.5×10^5 . Pressure fluctuation signal from one of the strips, upstream of the mean separation point showed a peak at 2.25 kHz (Fig. 2(a)). The mean separation point was located at about 79° from the forward stagnation point of the cylinder. When two transducer strips, located between 72° and 74° from the forward stagnation point, were excited in phase with a sinusoidal signal at 2.25 kHz, the mean separation point moved downstream to about 106° . These results are shown in Fig. 2(b). The movement of the separation point is seen in the mean pressure distribution plot. Integration of the mean pressure profiles showed a reduction in pressure drag of about 12.4%. In addition to the delay in separation, a hot wire velocity measurement in the wake showed that the vortex shedding frequency of 25-Hz was severely attenuated (Fig. 3).

Since the Reynolds numbers for which changes in flow separation could be detected ranged from 10^5 to 1.58×10^6 , it was suspected that the Acoustosurf was modifying the laminar-turbulent transition process. Experiments were repeated with a tripped boundary layer. Once again, excitation at 2.25 kHz of the same two strips resulted in a 20% reduction in the pressure drag (Fig. 4). The difference in this

case was that the pressure in the wake increased as a result of the excitation. The details of these experiments have been reported by Sinha and Pal (1994), and in the M.S. thesis by Pal (1994). Initially, it was believed that the acoustic radiation from the Acoustosurf was the primary perturbation mechanism (and hence the name "Acoustosurf"). However, subsequent observations have indicated that surface compliance effects play a predominant role. Smoke flow visualization was used to confirm the earlier studies. A downstream movement of the separation point is seen for flows both in the absence and presence of tripping (see Figs. 5 and 6). Flow visualization also showed that the boundary layer responded nearly instantaneously with the excitation. The effects of excitation were found to be reversible. This showed the possibility of using the Acoustosurf as a means for switching large energy flows with a relatively small energy input. Around 1 micro-Watt of electrical power was needed to reduce the drag-induced power loss by about 10 W.

The next set of experiments were run on a 300-mm chord NACA 0012 airfoil. Figure 7 shows a schematic of the layout of the strips for this case. Once again, the strips indicated peaks in the sensed pressure fluctuations. Since more than one peak was observed in the pressure fluctuation signature, the strips were oscillated at each of these frequencies. The effect on flow separation was observed using smoke flow visualization. Experiments were run in a different subsonic wind tunnel (maximum speed about 45 m/s). Results were obtained for chord-based Reynolds numbers of 4.3×10^5 and 8.25×10^5 . In both cases, the Acoustosurf was able to reattach flows which had just separated. Figure 8 shows the smoke-flow visualization photographs for the higher Reynolds number case. The Acoustosurf was found to be ineffective in reattaching massively separated flows. These occurred at angles of attack greatly exceeding the stall angle. This is not surprising since reattachment of massively separated flows calls for rather drastic measures, which the Acoustosurf is incapable of providing. The details of this study have been reported by Banerjee (1995).

UNDERSTANDING THE FLOW SEPARATION CONTROL MECHANISM

In order to understand the control mechanism, the relationship between the signals sensed by the strips and the instabilities present in the flow was examined. A test was conducted by exciting a group of strips of the Acoustosurf in the airfoil experiments over a range of frequencies, while measuring velocities in the separated shear layer with a hot-film probe. The response of the hot-film velocity probe is shown in Fig. 9 for the lower Reynolds number case described in the previous section. Maximum changes in the mean and fluctuation velocities occurred at two frequencies (2-kHz and 4.75 kHz). Flow visualization revealed that the boundary layer could be made to reattach at both frequencies. However, only partial reattachment occurred at 2-kHz, while complete reattachment took place at 4.75-kHz.

A similar experiment was recently conducted by Whitehead, et al., (1995) on a 14% thick Clark-Y airfoil of 223-mm chord. At a Reynolds number of 3.4×10^5 , a frequency of about 5 kHz was needed to control flow separation. A continuous (as opposed to segmented strips) driven-wall transducer was used in the vicinity of the leading edge. The transducer was capable of producing surface oscillation amplitudes of about 10-nm. Since the Reynolds numbers, airfoil chords, transducer type and oscillation frequencies matched closely with the present experiments, the flow control physics was probably similar. Since the configuration and size of the wind tunnel (and test section) used by

Whitehead et al. (1995) was significantly different compared to the present case, acoustic resonance effects can be expected to play a minor role.

Separated shear layers are very sensitive to a wide array of disturbance frequencies (Oster and Wygnanski, 1982). Therefore, exciting the shear layer is probably the primary reattachment mechanism. If acoustic modes are unimportant, the transducer has to energize the shear layer by propagating disturbances through the attached boundary layer. Therefore, one has to focus on the plausible non-acoustic means by which a flexible wall transducer introduces disturbances into the attached pre-separation boundary layer. These are briefly examined below.

Figure 10 shows an idealized form of the form of surface deflection of the transducer as a result of internal driving. Based on the change in slope of the surface, at the edges of the deformed shape, two counter-rotating spanwise vortices of strengths in the order of v/b will be injected into the near-wall region of the boundary layer during each oscillation cycle. To be effective in modifying the spanwise vorticity, v/b has to be of the same order as the near-wall velocity gradient. Since v varies linearly with the oscillation amplitude (a) and frequency (f), the parameter (af/b) has to exceed a certain threshold for any change to take place. For a given boundary layer flow, at a given Reynolds number, this can be achieved by increasing the amplitude and frequency of wall oscillation and reducing the spacing between transducer strips. The second method of interacting with the boundary layer will be through direct modification of the streamwise momentum as a result of the wall velocity v . This mechanism will act on the flat portion of the deflected shape of the wall (Fig. 10). How the vorticity and velocity disturbances influence the separated shear layer is currently being studied. It is speculated that vortex pairing action (Oster and Wygnanski, 1982) plays a key role.

The mechanisms elucidated here directly influence transducer design. A flexible wall transducer which can be used to impart large velocity perturbations (large a and f) and large vorticity fluctuations (small c) is preferred. This forms the basis of the final EMEMS transducer.

THE FINAL EMEMS TRANSDUCER

The performance of the Acoustosurf transducer relies primarily on the dielectric properties and compressibility of the air trapped between the flexible surface and the conducting strips. The maximum displacement possible and the resulting surface velocity and acceleration are limited by the magnitude of this gap. The effective gap is determined mainly by the magnitude of surface roughness of the conducting strips. This also imposes limitations on the maximum electrical voltage that can be applied and the range of passive compliance of the flexible wall. The velocity of the wall can be increased by increasing the acceleration for sinusoidal driving. The acceleration of the wall can be increased by increasing the driving force and the driving force is directly proportional to the voltage and inversely to the square of the thickness of the dielectric.

One way of removing the above mentioned limitations is to replace the air dielectric with a microstructured elastomeric substrate. An EMEMS transducer developed by Whitehead and Bolleman (1995), based on the patent by Whitehead et al. (1989), is shown in Fig. 11. The transducer's microstructured elastomeric substrate consists of a set of strip shaped ridges and valleys. A scanning electron micrograph of the

substrate is shown in Fig. 12. The major cost of the transducer is in building the mold for the substrate, since it involves micromachining grooves with high accuracy. However, the production cost per unit area can be expected to be fairly low once the cost of the mold is amortized. Thus it may be economically feasible to cover large areas with this material. The peaks of the microstructured elastomer strips are made electrically conducting. Electrostatic attraction between the conducting metal plate on the surface and the shorter strips moves the metal plate by compressing the taller ridges and the air trapped within the grooves. The stiffness of the transducer and the force of actuation can be independently controlled by varying the properties of the elastomer and groove geometry. This design therefore allows considerable customizing in terms of the size of the area to be activated along with the requisite mechanical properties such as the displacement amplitudes and natural frequencies. Additionally it is much less prone to impact damage than comparable silicon based MEMS or piezo-electric devices.

Several possibilities exist in modifying the arrangement shown in Figure 11. If short wave lengths (low value of $(2b+c)$ in Fig. 10) are desired, the arrangement of Fig. 11 can be inverted, with the back side of the elastomer facing the flow. The elastomer can be molded to obtain overall thicknesses less than 10-microns. Another possibility is to use the microstructured metallized tip elastomer as the strips in the Acoustosurf design. In this design, flexural waves, of wavelengths less than the gaps between the strips (Fig. 1), can be generated by driving the edges of the unexcited portions of the transducer surface. Microstructuring the strips simply affords better control. If the vorticity generation mode described in the previous section has to be maximized, the metallic surface in Fig. 11 can be made into individual segments, such that the relative movement between adjacent strips can be utilized to make the dimension b in Fig. 10 infinitesimal. The effect of these designs on separating and non-separating boundary layer flows will be the subject of future investigations.

CONCLUSIONS

The objective of this work was to develop a means of controlling unsteady separating boundary layers through a wall mounted micro actuator-sensor array. The design had to be robust enough for use in harsh environments, such as on compressor blades of turbine engines. Based on these requirements an electrostatically driven flexible wall transducer has been fabricated. The limited amount of testing done to date indicates that the transducer is capable of delaying separation in transcritical and tripped supercritical flows on a cylinder.

The transducer interacts with the flow through both passive and active modes. The passive mode effect is seen, for example, in the asymmetry in the measured mean pressure profiles on the cylinder. A method for determining the optimum location and frequency of active excitation has been devised by using the passive mode transducer response as a diagnostic. This method often yields multiple solutions, as evidenced from tests on airfoils. Additional screening criteria need to be developed to identify the correct or most effective frequency.

The transducer could control marginal separation on the NACA 0012 airfoil at a Reynolds number close to a million. However, extrapolation of this technique to higher Re values cannot be assured until the action of the transducer on the flow is properly understood. Since the transducer could reattach separating flows using an extremely small amount of external power, it is believed that it was exploiting flow instabilities. While the exact mechanism of energy transfer between the

separating flow and the transducer is not yet very clear, it can be argued, based on existing experiments, that the acoustic radiation from the transducer probably plays an insignificant role in this process. The interaction of the wall motion with the flow can be characterized in terms of evolving coherent structures (Breuer, et al., 1989). In order to interact effectively at the scales of these structures for practical high-Re flows (Gad-el-Hak and Bandyopadhyay, 1994), miniaturization of the transducer elements will be needed. The primary modes of interaction seem to be the injection of spanwise vorticity and normal velocity fluctuations into the near wall region of the boundary layer. Since the most sensitive area of the flow is the separated shear layer, the perturbations introduced by the transducer probably lock on to one of the shear layer instability modes.

If vorticity injection is the predominant mode of interaction, transducers with extremely thin strips will be preferred. If adjacent wall segments of the transducer can be made to move relative to each other (i.e., normal to the wall), a large amount of vorticity can be introduced even with small oscillation velocities. In order to utilize this aspect of the transducer it is proposed that a design based on a microstructured elastomeric substrate be used. This is the EMEMS transducer which is the final concept arising out of this effort. Due to its mechanical simplicity, the cost of this transducer can be expected to be significantly lower compared to comparable micro-machined silicon devices. It can also be expected to be more rugged. Flow tests with the final EMEMS design have yet to be carried out.

ACKNOWLEDGEMENTS

The authors thank the sponsors of this work. The Air Force Office of Scientific Research supported the initial phase of this research through Grant No. AFOSR-91-0410. Part of the subsequent research has been funded by Grant Nos. DAAH 04-94-G-0268 and DAAH-04-93-G-0451 from the Army Research Office. A final note of thanks is due to Dr. Lorne Whitehead and Mr. Brent Bolleman of GMW Spekertape, Canada for sharing their research experiences on transducer development.

REFERENCES

- Ahuja, K. K., and Burrin, R. H., 1984, "Control of Flow Separation by Sound", AIAA Paper 84-2298.
- Bandyopadhyay, P.R., 1995, "Microfabricated Silicon Surfaces for Turbulence Diagnostics and Control", Proceedings, ACTIVE 95, Newport Beach, CA, pp. 1327-1338.
- Banerjee, D., 1995, "An Experimental Investigation of Flow Separation Control using an Acoustic Active Surface", M. S. Thesis, University of Mississippi, Oxford, MS.
- Breuer, K. S., Haritonidis, J. H., and Landahl, M. T., 1989, "The Control of Transient Disturbances in a Flat-Plate Boundary Layer through Active Wall Motion", Physics of Fluids A, Vol 1, No. 3, pp. 574-582.
- Bushnell, D. M., Hefner, J. N., and Ash, R. L., 1977, "Effect of Compliant Wall Motion on Turbulent Boundary Layers", Physics of Fluids, Vol. 20, No. 10, Pt. II, pp. S31-S48.
- Gad-el-Hak, M., and Bushnell, D. M., 1991, "Separation Control: Review", ASME Journal of Fluids Engineering, Vol. 13, pp. 5-30.
- Gad-el-Hak, M., 1989, "Flow Control", Applied Mechanics

Review, Vol. 42, No. 10, pp. 261-293.

Gad-el-Hak, M., 1994, "Interactive Control of Turbulent Boundary Layers: A Futuristic Overview", AIAA Journal, Vol. 32, No. 9, pp. 1753-1765.

Gad-el-Hak, M., and Bandyopadhyay, P.R., 1994, "Reynolds Number Effects in Wall-Bounded Turbulent Flows", ASME Applied Mechanics Reviews, Vol. 45, No.8., pp. 307-366.

Kramer, M. O., 1960, "Boundary Layer Stabilization by Distributed Damping", Journal of the American Society of Naval Engineers, Vol. 72, pp. 25-33.

McMichael, J. M., 1996, "Progress and Prospects for Active Flow Control using MEMS", AIAA Paper No. 96-0306.

Oster, D., and Wagnanski, I., 1982, "The Forced Mixing Layer between Parallel Streams", Journal of Fluid Mechanics, Vol. 123, pp. 91-130.

Padmanabhan, A., Goldberg, H. D., Breuer, K. S., and Schmidt, M. A., 1995, "A Silicon Micromachined Floating Element Shear Stress Sensor with Optical Position Sensing with Photodiodes", Technical Digest, 8th International Conference on Solid-state Sensors and Actuators, and Eurosensors IX., pp. 436-439.

Pal, D., 1993, "An Experimental Characterization of the Interaction Mechanisms for Flow Separation Control using Sound", M. S. Thesis, University of Mississippi, Oxford, MS.

Sinha, S. K., and Pal, D., 1994, "Controlling Unsteady Separation with Acoustic Active Surfaces", AIAA Paper 94-0183.

Sinha, S. K., and Pal, D., 1993, "Optimizing the use of Acoustic Perturbation to Control Unsteady Boundary Layer Separation", ASME Fluids Engineering Conference, Washington D.C., (FED VOL. 157), pp. 33-46.

Sinha, S. K., 1996, "The ACOUSTOSURF: a Multi-Element Acoustic Active Surface for Flow Separation Control" (Patent pending).

Tsao, T., Liu, C., Tai, Y. C., and Ho, C. M., 1994, "Micromachined Magnetic Actuators for Active Fluid Control", Proc. of ASME Appl. of Microfabrication to Fluid Mechanics, FED-Vol. 197, pp. 31-38.

Weinstein, L. M., 1981, "Effect of Driven Wall Motion on a Turbulent Boundary Layer", IUTAM Symposium on Unsteady Turbulent Shear Flows, Toulouse, France, pp. 58-66.

Wehrmann, O. H., 1965, "Tollmien-Schlichting Waves Under the Influence of a Flexible Wall", Physics of Fluids, Vol. 8, pp. 1389-90.

Whitehead, L. A., Graham, D. J., Moore, F. A., Lake, R., Bolleman, B. J., Dunwoody, A. B., and Fitzsimmons, J., 1995, "Investigation of Boundary Layer Flow Separation Control by Airfoil Surface Vibration", private communication.

Whitehead, L. A., et al., 1989, "Elastomer Membrane Enhanced Electrostatic Transducer", U.S. Patent 4,885,783.

Whitehead, L. A., and Bolleman, B. J., 1995, "Microstructured Elastomeric Electromechanical Film Transducer", (Draft Preprint).

Williams, D., Acharya, M., Bernhardt, J., and Yang, P., 1991, "The Mechanism of Flow Control on a Cylinder with the Unsteady Bleed Technique", AIAA Paper 91-0039.

Zaman, K. B. M. Q., 1992, "Effect of Acoustic Excitation on Stalled Flow over an Airfoil", AIAA Journal, Vol. 30, No. 6, pp. 1492-1499.

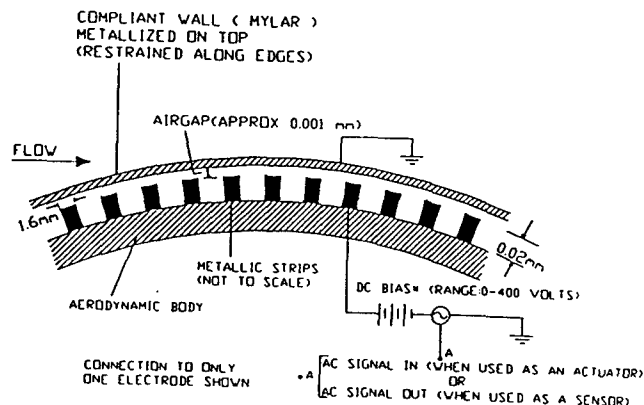


Figure 1. Schematic of the Acoustosurf.

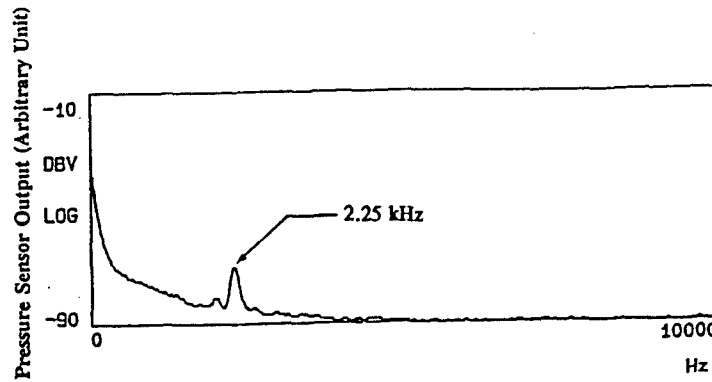
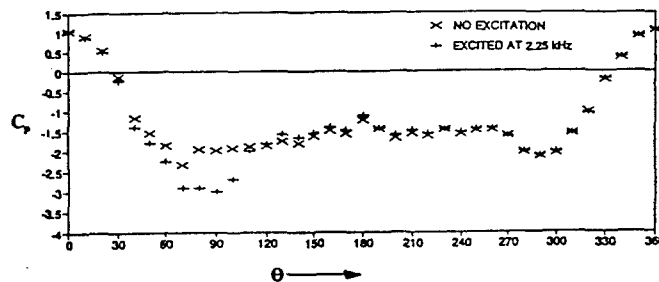


Figure 2(a). The pressure-fluctuation spectrum of the unexcited boundary layer on a cylinder at $Re = 1.5 \times 10^5$ sensed by an Acoustosurf strip located at 78° from forward stagnation.



$$C_p = \text{Coefficient of Pressure} = (p - p_\infty) / (0.5 \rho U_\infty^2)$$

Θ = Angular Position from Forward Stagnation Point

Figure 2(b). Surface static-pressure distribution around cylinder under unexcited and excited conditions. Acoustosurf strips between 72° and 74° from forward stagnation subject to 10-volts amplitude sinusoidal excitation at 2.25 kHz. $Re = 1.5 \times 10^5$.

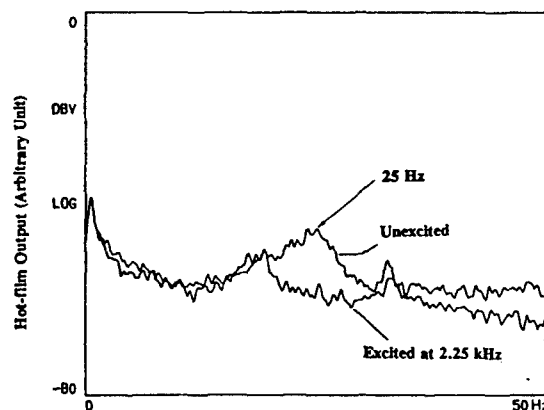
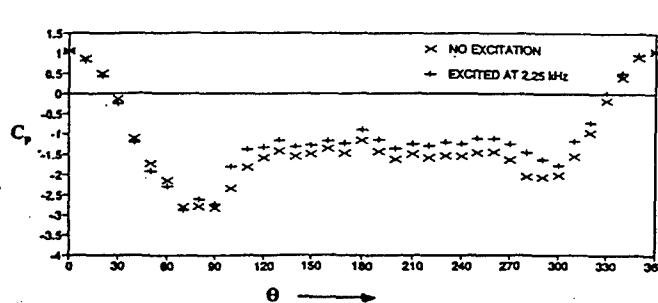


Figure 3. Suppression of vortex shedding by excitation at 2.25 kHz using the Acoustosurf. Velocity spectra of cylinder wake under unexcited and excited states. Prominent peak at 25 Hz under unexcited condition. Excitation at 72° - 74° . Measurement at 110° and 10-mm away from cylinder surface. $Re = 1.5 \times 10^5$.



$$C_p = \text{Coefficient of Pressure} \\ = (p - p_\infty) / (0.5 \rho U_\infty^2)$$

θ = Angular Position from Forward Stagnation Point

Figure 4.

Surface static-pressure distribution around cylinder under unexcited and excited conditions. Acoustosurf strips between 72° and 74° from forward stagnation subject to 10-volts amplitude sinusoidal excitation at 2.25 kHz. Flow was tripped at 35° from forward stagnation. $Re = 1.5 \times 10^5$.



Figure 5(a).

Smoke-flow visualization of the untripped flow in absence of Acoustosurf excitation. $Re = 1.5 \times 10^5$.



Figure 5(b).

Smoke flow visualization of the untripped flow with Acoustosurf excitation at 72° - 74° and 2.25 kHz. $Re = 1.5 \times 10^5$.



Figure 6(a). Smoke flow visualization of the tripped flow in absence of Acoustosurf excitation. $Re = 1.5 \times 10^5$. Artificial flow tripping at 35° from forward stagnation.



Figure 6(b). Smoke flow visualization of the tripped flow with Acoustosurf excitation at 72° - 74° and 2.25 kHz. $Re = 1.5 \times 10^5$. Artificial flow tripping at 35° from forward stagnation.

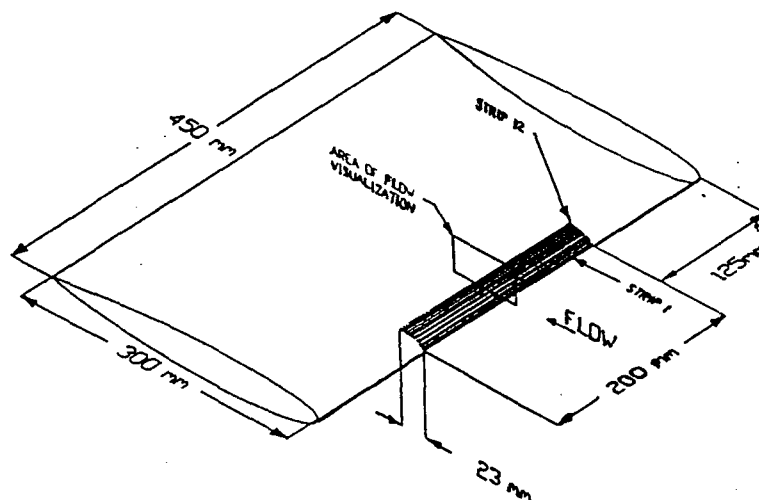


Figure 7. Schematic of airfoil showing Acoustosurf strip layout.

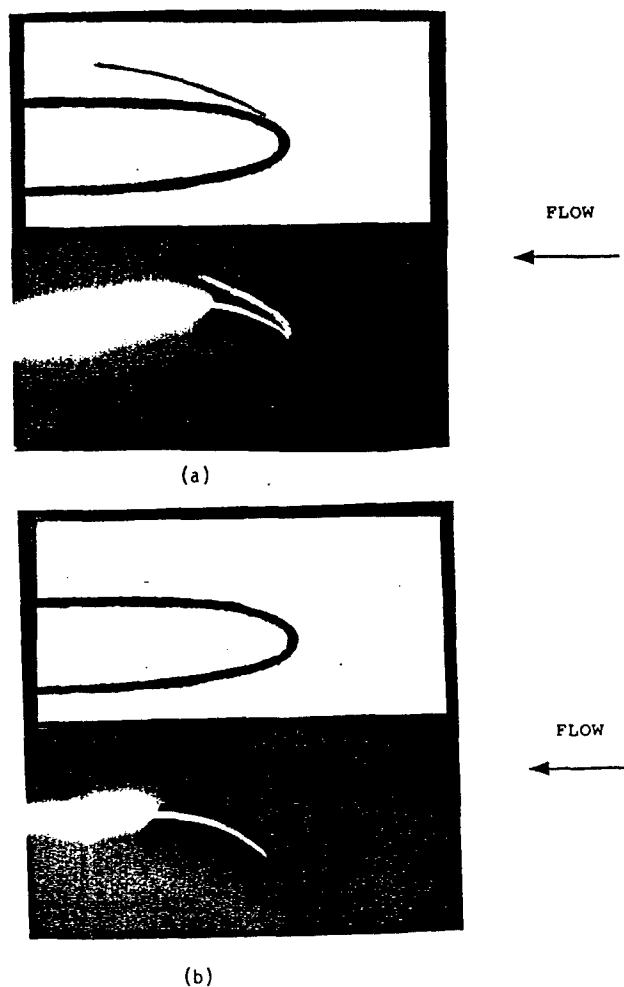


Fig 8. Smoke flow visualization of reattachment of separated flow over an NACA-0012 airfoil at an angle of attack of 14° and at an Re of 8.25×10^5 .
(a) unexcited (b) excited at 2-kHz. Interpretations are shown for clarity.

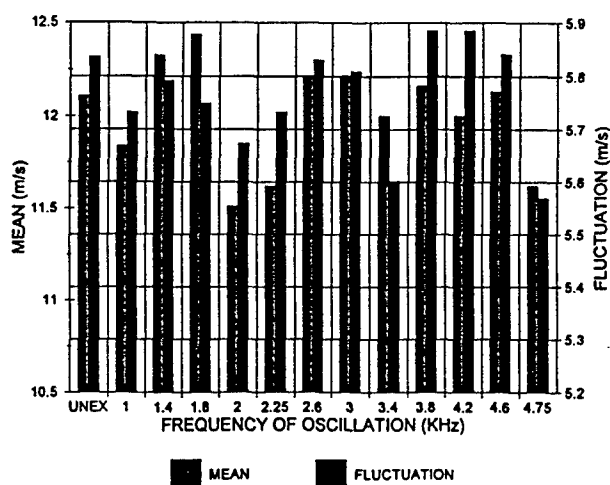


Figure 9. Effect of excitation frequency on NACA-0012 airfoil wake velocities (mean and fluctuation). Measurement at hot-film sensor at $x/c = 1.55$, $y/c = 0.083$. Multi-element excitation at airfoil leading edge ($x/c = 0 - 0.02$). $Re = 4.3 \times 10^5$.

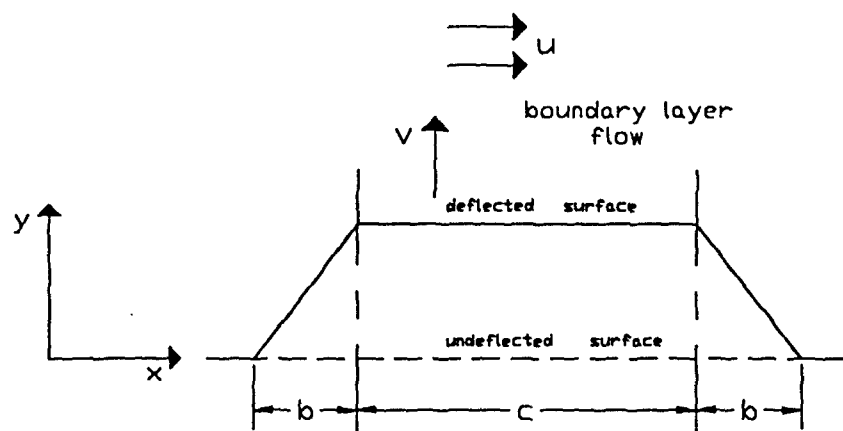


Figure 10. Idealized form of surface deformation.

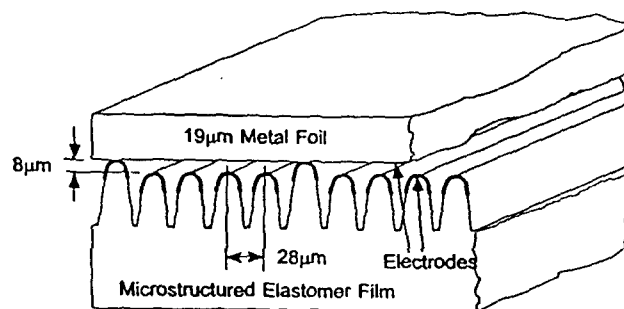


Figure 11. Microstructured elastomeric transducer prototype.

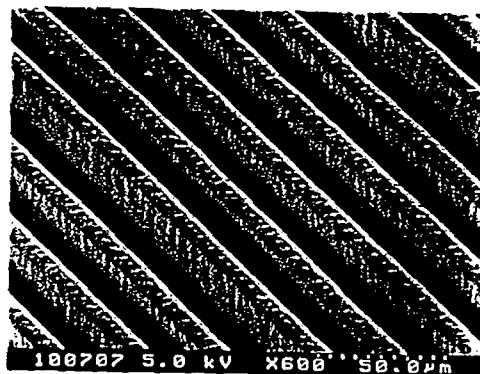


Figure 12. Scanning electron micrograph (x600) of the Microstructured elastomer surface used in the prototype.

A COMPLIANT WALL SENSOR ARRAY FOR DETECTING PRESSURE FLUCTUATION SIGNATURES IN SEPARATING BOUNDARY LAYERS

Dipankar Pal¹, Sumon K. Sinha², Debjyoti Banerjee³, Chuck Baker⁴ and Mukesh Pandey⁵

Mechanical Engineering Department

University of Mississippi

University, Mississippi 38677

Phone : (601) 232-5374, Fax : (601) 232-5374

All Communications should be addressed to Dr. Sumon K. Sinha at the above address.

Introduction :

Controlling unsteady separating flows is of importance in a wide variety of aerodynamic and hydrodynamic applications. These range from alleviating the effects of dynamic stall on helicopter rotors to delaying the onset of cavitation in pump impellers. A strategy for controlling unsteady separation optimally is to devise sensors which can indicate where and when an attached boundary layer is about to separate. A small disturbance of the appropriate type, such as controlled blowing or suction, can then be effectively utilized to prevent or delay separation.

An oncoming separation may be detected by sensing wall shear stress variation, near-wall velocity profiles or flow-induced wall pressure fluctuations. In this study, wall pressure fluctuations were sensed. An array of compliant wall sensors was used to estimate characteristic pressure fluctuations in typical

unsteady and steady separating boundary layers on a cylinder and an NACA-0012 airfoil in wind-tunnel experiments. The array of sensors was designed such that the compliant wall elements responded primarily to the flow induced wall pressure fluctuations. The intent was to capture the spatial and temporal variations of wall pressure fluctuations from the output signatures of the compliant wall elements. The spatial and temporal correlations of the fluctuation signals can be expected to yield the proper phase relation of the unsteadiness^{[1],[2]}. Such information can then be used in a feedback control strategy^[3] for the control of stalling flows. The advantage of this method is that measurements can be nearly instantaneous if the signal processing time is minimized. In comparison, the responses of shear sensitive liquid crystal coatings^[4] or pressure sensitive paints generally limit their applications to relatively slower or quasi-steady phenomena.

¹ Research Assistant, Student Member AIAA

² Associate Professor, Senior Member AIAA

³ Research Assistant, Presently at Department of Mechanical, Aerospace and Nuclear Engineering, University of California, Los Angeles

⁴ Research Assistant, Student Member AIAA

⁵ Research Assistant, Student Member AIAA

Additionally, the sensor array is simple in design and does not require sub-surface instrumentation as needed for pin-hole microphones.

In this study, the nominally two-dimensional geometry of the sensors allowed the measurement of streamwise variation of the fluctuation field only, though incipient separation is commonly characterized by the formation of three-dimensional cell-like structures. In case of two-dimensional steady separation^[5], the streamwise length scale of these structures in the sublayer is $O(Re^{-3/8})$, whereas the boundary layer thickness is $O(Re^{-1/2})$. For unsteady flow separation on an impulsively started circular cylinder, the streamwise scale of the near-separation structures is $O(Re^{-3/11})$. Therefore, the size of the sensor elements has to be small enough to adequately resolve the spatial features of pressure fluctuations at these scales.

Construction of the Sensor-Array and Measurement Technique :

The array of sensors^[6] consisted of a thin flexible dielectric (Mylar) membrane with its outer surface made electrically conductive by depositing aluminum (Figure 1.). The thicknesses of the membrane was 6 microns. The membrane was stretched over an array of thin and nearly flush-mounted metallic strips. These sensing elements had dimensions of 1-mm x 300-mm. The periphery of the flexible rectangular membrane was glued onto the aerodynamic surface so that just enough tension was maintained to avoid slackness of the membrane. The metallized face of the flexible wall was electrically insulated from the metallic sensing elements by virtue of the non-conducting Mylar. The strip-shaped sensor elements can alternatively be built by etching out a thin metal-clad polyamide sheet, which can then be mounted on the aerodynamic surface. Either way, the metallic strips and the

thin air-gaps between consecutive elements constitute the substrate of the compliant wall.

A D.C. bias voltage (400 volts for the present study) was applied between each of the sensing elements and the outer surface of the flexible wall. It helped in keeping the wall close to the elements by electrostatic attraction. This attractive force and the inter-element spacing define the stiffness and damping characteristics of the capacitor-type sensors. The maximum permissible bias voltage depended on the electrical breakdown characteristics of the Mylar membrane-air gap combination. When the array of sensors was mounted on an aerodynamic surface, the unsteady flow caused the membrane to vibrate. The output voltage from each strip-shaped sensor element, with the D.C. bias isolated, was proportional to the change in capacitance for the particular sensor. The wall pressure fluctuations above each strip are primarily responsible for changing the cell capacitance by inducing fluctuations in the air gap between the Mylar and the metallic strips.

Flows over passive compliant walls often result in the occurrence of surface instabilities in the form of static divergence or traveling wave flutter^[7]. The frequency and mode of the wall vibration depends on the coupling of the flow with the compliant wall. Therefore, the response of the sensors to flow-induced surface instabilities play a crucial role. The effect of wall shear-stress on the measurement of pressure fluctuations is minimal as long as the D.C. bias voltage is high enough to prevent shear-induced buckling of the compliant wall. Higher order interactions may occur, but have been ignored in this work.

Experiments :

The first set of experiments involved unsteady separating flow over a 155-mm diameter circular cylinder in a subsonic wind-

tunnel (Figure 2). The Reynolds number, based on cylinder diameter, was varied between 1.2×10^5 to 1.7×10^6 . The unsteady nature of separation at these subcritical Reynolds numbers was dominated by the large amplitude oscillations due to vortex-shedding ($f_s \approx 25$ Hz). The mean point of separation was at $\theta = 82^\circ$, where θ is the angle measured from the forward stagnation point of the cylinder. The sensor array was mounted at an angular location of $\theta = 65^\circ$ - 100° , so that the variation of pressure fluctuations could be observed near the point of separation.

The next set of experiments investigated the flow over a 300-mm chord NACA-0012 airfoil in a higher velocity closed circulation wind-tunnel. The sensor array covered the region between $x/c = 0$ to $.08$ of the airfoil and comprised of twelve 1-mm wide sensor elements as shown in Figure 3. The chordal Reynolds number (Re_c) was varied between 4×10^5 to 8.5×10^5 . The lift-coefficient (C_L) increases monotonically with angle of attack (α) at this range of Reynolds numbers till the stall angle is reached. The angle of attack was set such that it was just below the steady stall angle for the particular Re_c . Pressure-fluctuations near the leading edge were studied.

Results :

Preliminary results showed encouraging prospects for the use of compliant wall sensors in separation study. Figure 4 shows the time-averaged spectrum of wall pressure fluctuations, as measured by a sensor element on the cylinder surface at $\theta = 78^\circ$. The broadband peak at 2.25 kHz points to a separation instability due to fluctuations in pressure. The rms of the surface pressure fluctuations increased as the mean point of separation was approached. The characteristic peak around 2.25 kHz was detectable in strips located from $\theta = 78^\circ$ to $\theta = 82^\circ$. In terms of

streamwise spacing, the $O(Re_c^{-3/11})$ structure corresponds to an angular spacing of 4.5° . Hence, these experiments showed that this feature could be used to detect the separation location, as long as the sensor strips had adequate spatial resolution in the streamwise direction. Additionally, the instability signature at 2.25 kHz could be successfully used as a perturbation frequency for transitional flow control over the cylinder by Sinha and Pal^[8].

The time-averaged pressure fluctuation spectrum on the suction surface of the NACA-0012 airfoil is shown in Figure 5. The Reynolds number was 4.3×10^5 . At an angle of attack of 11° , the spectrum shows that high frequency fluctuations start dominating the flow near the separation point ($x/c = 0.06$). Flow visualization revealed the onset of separation at $\alpha \approx 12^\circ$. In their experimental study of wall pressure fluctuations (p') in a separating turbulent boundary layer, Simpson et al.^[9] suggested that p' increases till the point of detachment and decreases downstream. Similar variation of pressure fluctuations could be observed for the pre-stalled flowfield near the leading-edge of the airfoil.

In order to determine whether the frequency peaks sensed in this manner had any significance in terms of exciting the just separated boundary layer to achieve reattachment, the transducer elements near the leading edge were used as wall actuators by applying an external alternating voltage at various frequencies. The effect of excitation was sensed using a hot film sensor downstream of the excitation point (Figure 6). Maximum changes were noted at 2-kHz and 4.75-kHz. These frequencies are close to the frequencies of the two major pressure fluctuation peaks observed in Figure 5. However, they do not exactly coincide. Flow visualization revealed that excitation at 2-kHz resulted in intermittent reattachment, while a complete reattachment occurred at 4.75-kHz.

Work in progress :

On the basis of the information obtained in the experiments on the circular cylinder and the statically stalled airfoil, experiments are currently underway for identifying wall-pressure fluctuation precursors on flows over pitching airfoils. A new test section incorporating a pitching NACA-0012 airfoil has been built and is currently undergoing qualification tests. A photograph of the test section is shown in Figure 7. A microcomputer-based data acquisition system incorporating eight 8-bit 20-MHZ A/D boards has been installed to capture data simultaneously from eight transducer strips. The high speed is essential to sample adequate data points around the instant of separation. The separation process is being monitored using smoke flow visualization. The approximate α at which the flow is observed to separate for a given pitch-rate- Re_c combination is being used to trigger the data acquisition process. Figure 8. shows a set of preliminary pressure fluctuation data obtained in this manner.

Following the scaling laws developed by Smith^[5], the final boundary layer "eruption" process, which initiates dynamic stall on an airfoil, has a streamwise length scale of $O(Re_c^{-5/11})$. For the 300-mm chord NACA-0012 airfoil this corresponds to a streamwise length of about 0.6-mm at $Re_c = 8.5 \times 10^5$. Hence the strips in the transducer need to be less than 0.2-mm wide to capture the pressure fluctuation signature of the eruption process on two consecutive strips. This work is currently in progress and results are expected in time for preparation of the final manuscript.

Conclusions

A compliant wall transducer comprising of an array of strip shaped sensors has been used to sense pressure fluctuations

just prior to and during unsteady and steady boundary layer separation. On circular cylinders at subcritical to critical Reynolds numbers, the sensors detected a characteristic pressure fluctuation frequency. This frequency was found to have significance in reattaching the separated shear layer. The amplitude of pressure fluctuation signals from the array of sensor strips directly indicated the location of the separation point. Similar data was also obtained from the sensors when used on an airfoil operating just under stalling conditions. Experiments are currently underway to explore the use of this technique to obtain precursors to dynamic stall on pitching airfoils. A time-space footprint of wall pressure fluctuation signals is expected. While the $O(Re_c^{-5/11})$ type streamwise scaling law may not be valid for Re_c greater than 5×10^5 , it is being used to size the transducer elements. The final results may be affected by traveling wave type instabilities arising out of the unsteady flow over the compliant wall.

Acknowledgments :

The authors acknowledge support from the U.S. Army Research Office for supporting this research through Grant numbers DAAH 04-93-G-0451 and DAAH 04-94-G-0268. The grants are being administered by Dr. Thomas Doligalski, whose mentorship is also gratefully acknowledged.

References :

- [1] Farabee, T.M., and Casarella, M.J., "Wall Pressure Fluctuations beneath a Disturbed Turbulent Boundary Layer", International Symposium on Flow Induced Vibration and Noise", 1988, Vol.6, pp. 121-135.
- [2] Wilczynski, V., and Casarella, M.J., "Correlations between Organized Turbulent Structures and Wall Pressure Fluctuations",

NCA-Vol. 13, Symposium on Flow induced Vibration and Noise, Vol. 3, 1992.

[3] Hendricks, G.J., and Gysling, D.L., "Theoretical Study of Sensor-actuator Schemes for Rotating Stall Control", Journal of Propulsion and Power, Vol. 10, No. 1, 1994, pp. 101-109.

[4] Reda, D.C., "Observations of Dynamic Stall Phenomena using Liquid Crystal Coatings", AIAA Journal, Vol. 29, No.2, 1990, pp. 308-310.

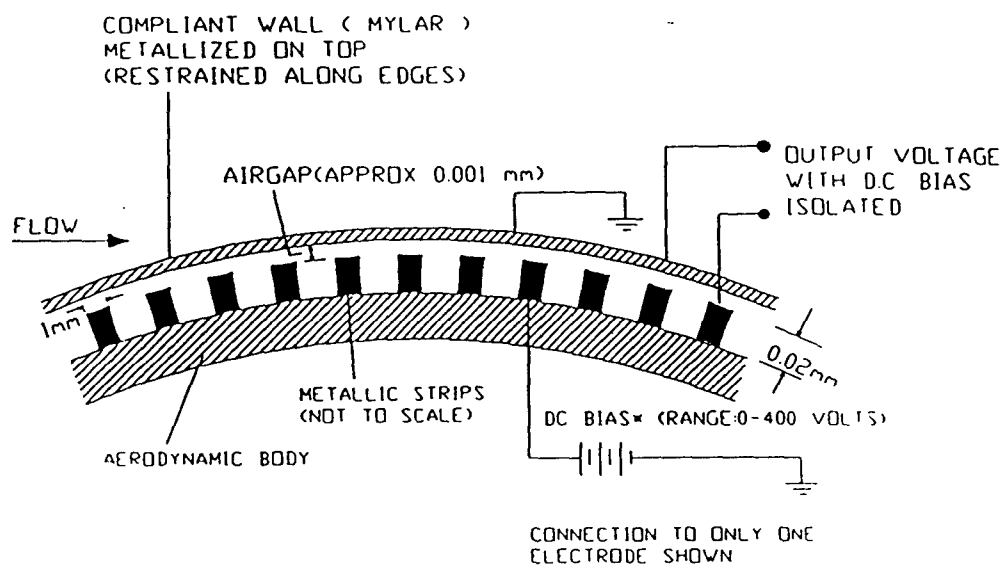
[5] Smith, F.T., "Steady and Unsteady Boundary-Layer Separation", Annual Review of Fluid mechanics, Vol. 18, 1986, pp. 197-220.

[6] Sinha, S.K., "The ACOUSTOSURF - a Multi-Element Acoustic Active Surface for Flow Separation Control", Patent pending.

[7] Carpenter, P.W., and Garrad, A.D., "The Hydrodynamic Stability of Flow over Kramer-type Compliant Surfaces. Part 2. Flow-induced Surface Instabilities", Journal of Fluid Mechanics, Vol. 170, 1986, pp. 199-232.

[8] Sinha, S.K., and Pal, D., "Controlling Unsteady Separation with Acoustic Active Surfaces", AIAA Paper No. 94-0183.

[9] Simpson, R.L., Ghodbane, M., and McGrath, B.E., "Surface Pressure Fluctuations in a Separating Turbulent Boundary Layer", Journal of Fluid Mechanics, Vol. 177, 1987, pp. 167-186.



* NOTE Natural frequency depends on membrane tension and DC bias voltage

SIDE VIEW

Figure 1. Schematic of the compliant wall sensor array.

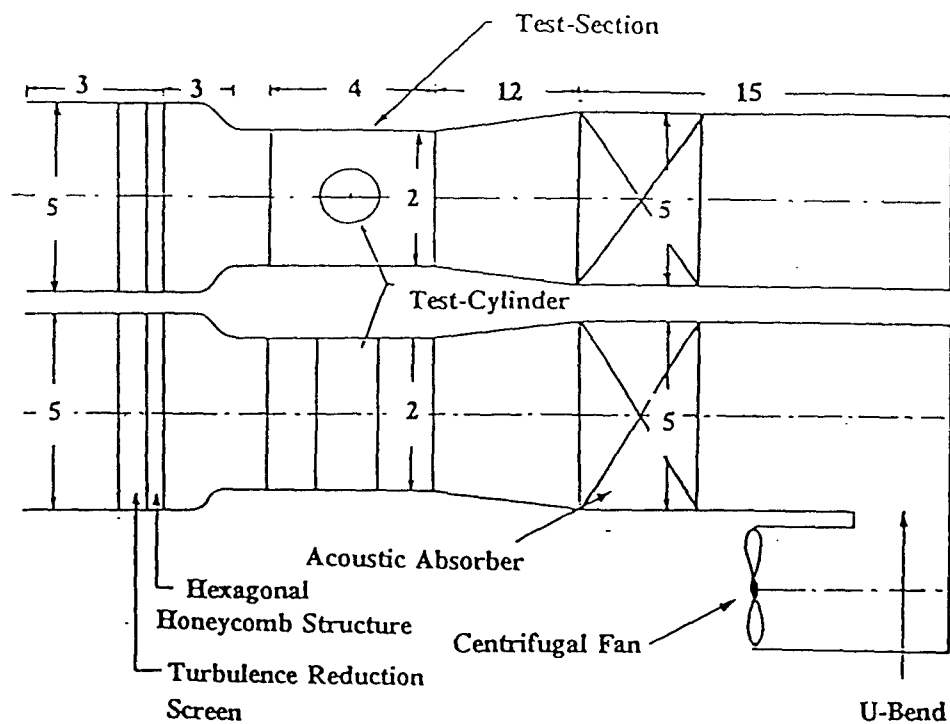


Figure 2. Wind-tunnel testing facility. All dimensions in ft.

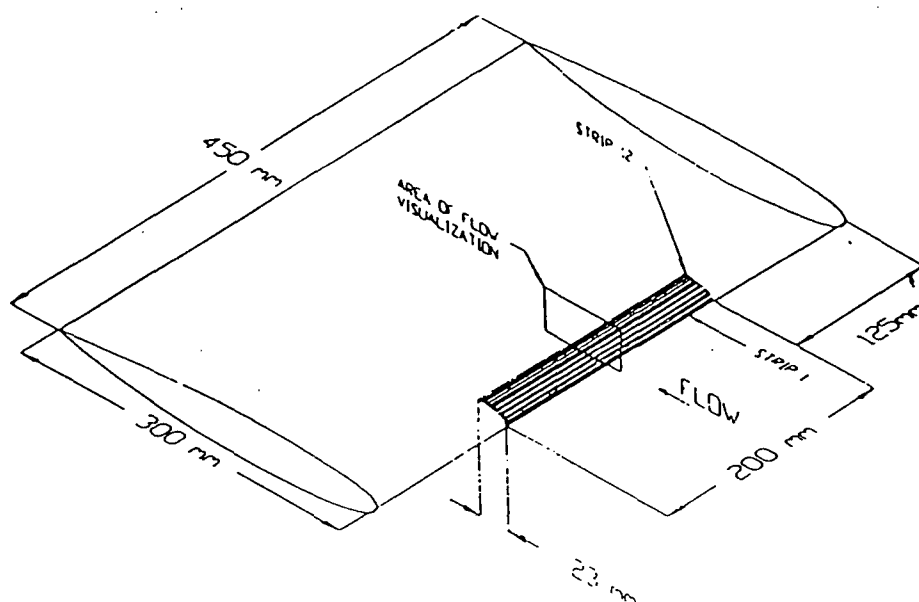


Figure 3. Arrangement of the compliant wall sensor array on NACA-0012 airfoil.

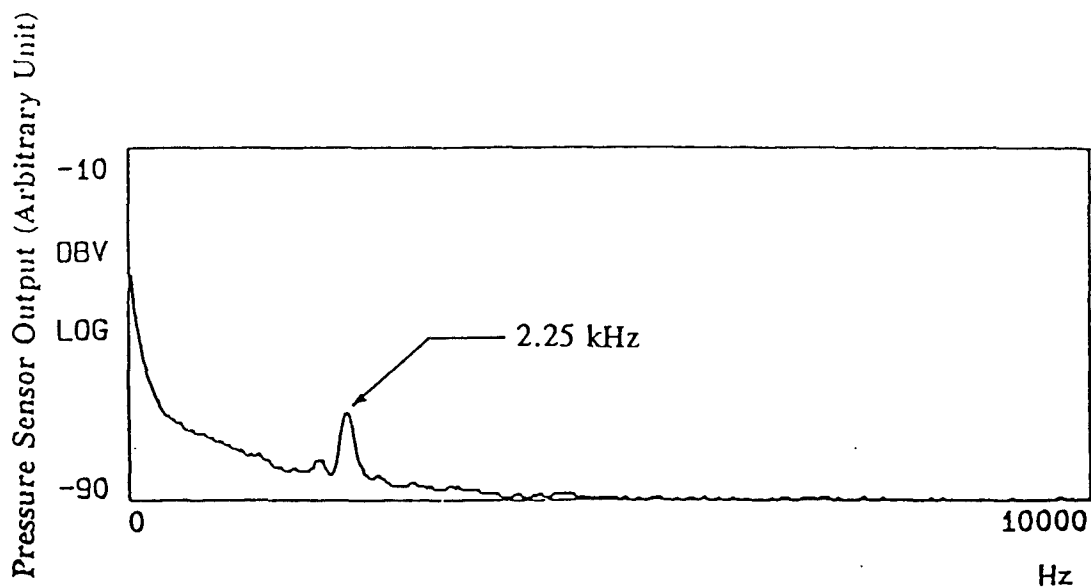


Figure 4. Time-averaged pressure fluctuation spectrum of pre-separation boundary layer in the absence of compliant wall actuation. $Re_d = 1.5 \times 10^5$. Measurement location : $\theta = 78^\circ$.

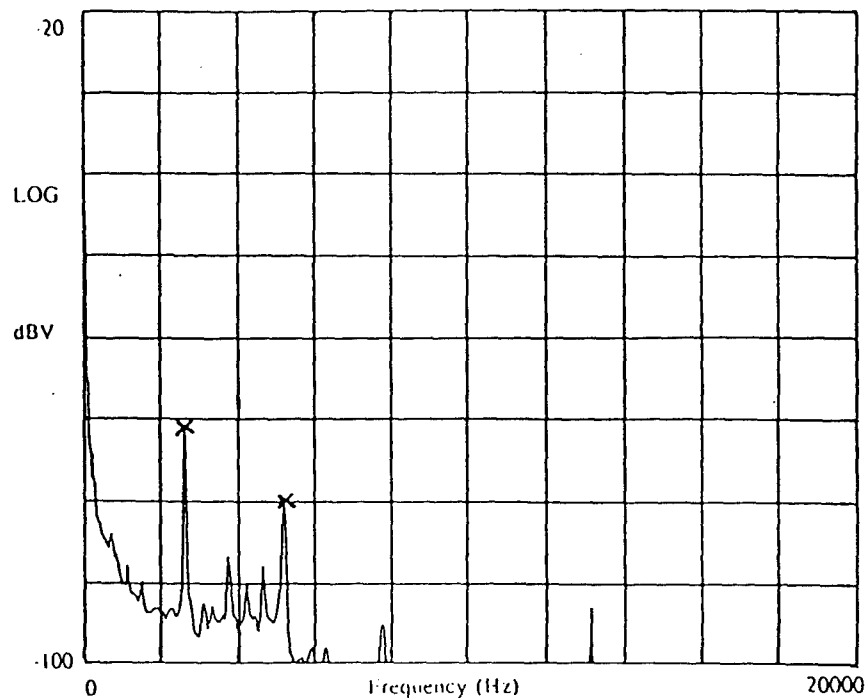


Figure 5. Time-averaged pressure fluctuation spectrum on the suction surface of the steady NACA-0012 airfoil ($x/c = 0.067$). $\alpha = 11^\circ$. $Re_c = 4.3 \times 10^5$.

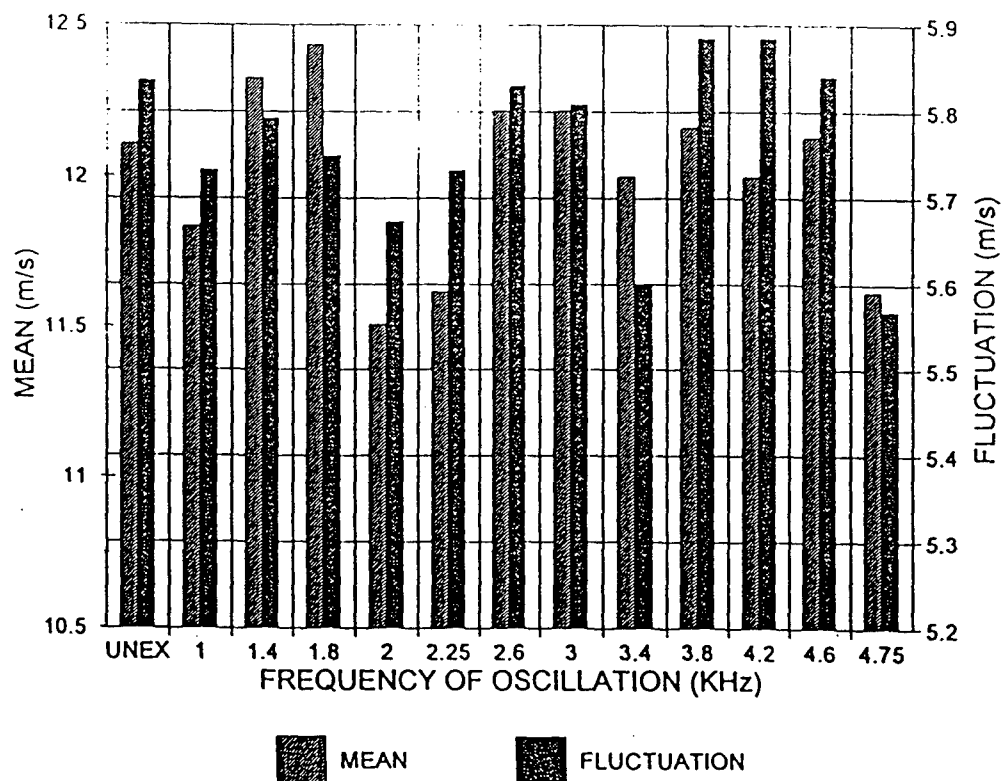


Figure 6. Effect of excitation frequency on NACA-0012 airfoil wake velocities (Mean and Fluctuation). Measurement with hot-film sensor at $x/c = 1.55$, $y/c = +.083$. Multi-element excitation at airfoil leading edge ($x/c = 0-0.02$). $Re_c = 4.3 \times 10^5$.

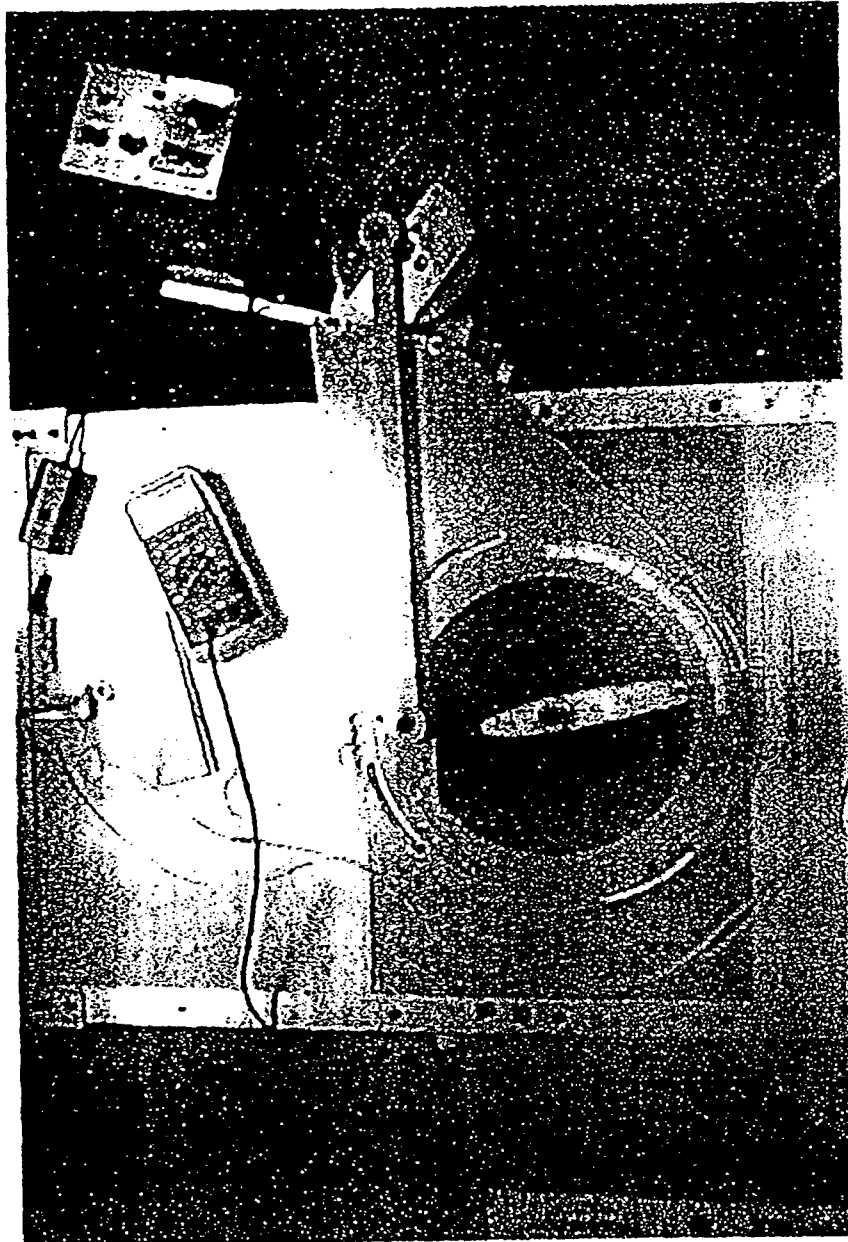


Figure 7. Dynamic stall facility in the closed circulation wind-tunnel.

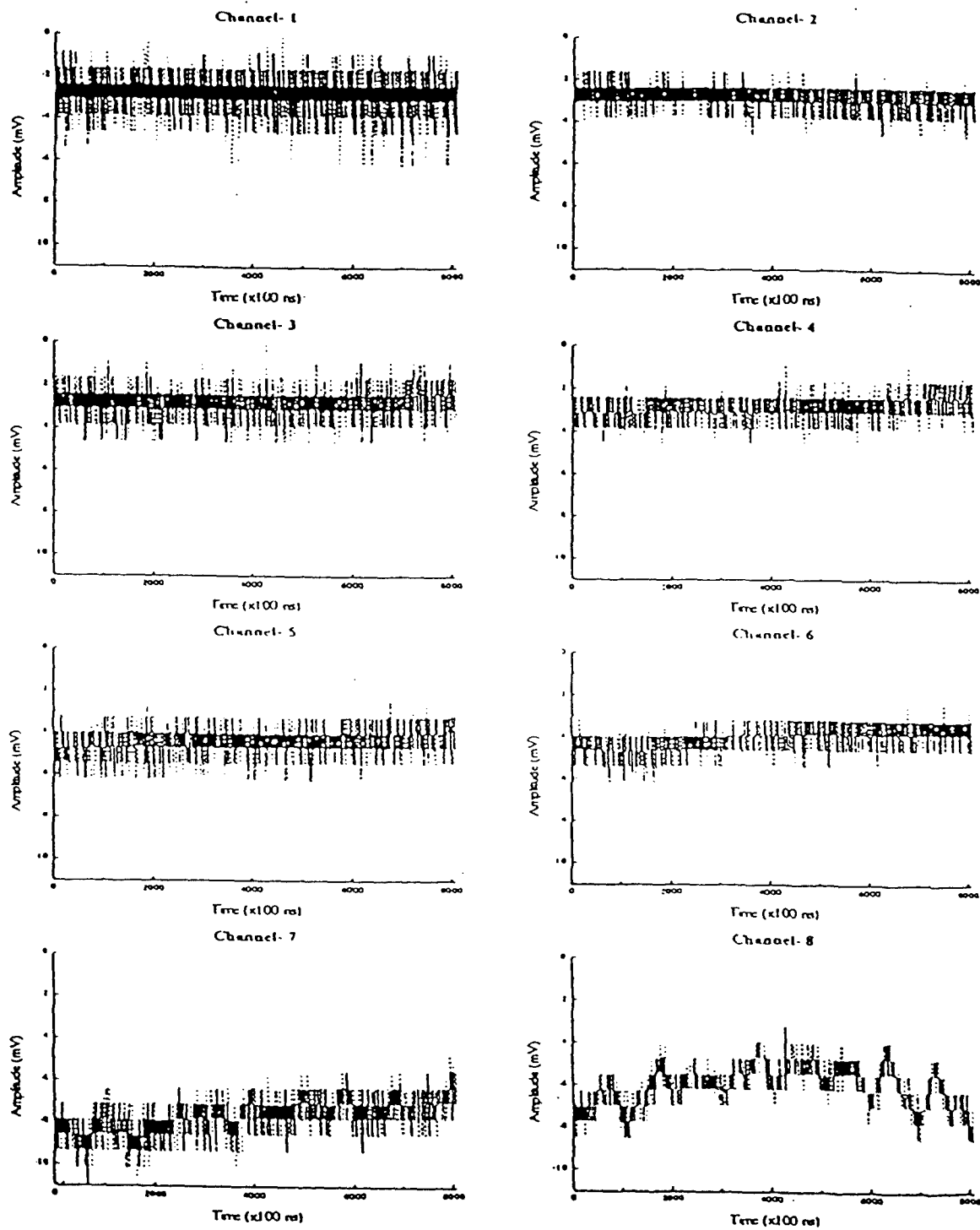


Figure 8. Preliminary pressure fluctuations data obtained from eight consecutive sensor elements on the pitching NACA-0012 airfoil. $Re_c = 9 \times 10^5$. Reduced frequency ($\omega c/U_\infty$) = 0.03.

CONTROLLING AN UNSTEADY SEPARATING BOUNDARY LAYER ON A CYLINDER WITH AN ACTIVE COMPLIANT WALL

D. Pal¹ and S. K. Sinha²

Department of Mechanical Engineering

The University of Mississippi

University, Mississippi 38677

Phone : (601) 232-5374, Fax : (601) 232-7219

All communications should be addressed to Dr. Sumon K. Sinha at the above address.

ABSTRACT

An active compliant wall, consisting of an array of nominally two-dimensional actuating and sensing transducers, has been used to control the unsteady separating flow over a circular cylinder. The flow Reynolds number, based on cylinder diameter, was varied between 1.2×10^5 and 1.7×10^5 . This range of Reynolds numbers corresponds to the transition from subcritical to critical flow over a rigid cylinder¹. The forced vibration of the entire compliant wall and the resulting acoustic radiation from the actuator element were observed to modify the separation characteristics of the near-parallel oscillatory flow. The compliant wall actively interacts with naturally occurring instabilities of the flow at this range of transitional Reynolds numbers^{1,2}. The actuation was found to delay separation during the boundary layer transition process. The forcing resulted in the reduction in root mean square velocity fluctuations, a modification in the wake velocity profiles, and a reduction in mean pressure drag.

NOMENCLATURE :

C_L = Lift coefficient
 $= 2L/(\rho U_\infty^2)$
 C_p = Pressure coefficient
 $= (p - p_\infty)/0.5\rho U_\infty^2$
 d = Diameter of the cylinder
 $= 152 \text{ mm}$
 l = Length of cylinder
 H = Height of test section
 f_a = Acoustic excitation frequency
 f_v = Vortex shedding frequency
 L = Lift force

p = Surface static pressure
 p_∞ = Upstream static pressure
 Re_d = Reynolds Number based on d
 $= U_\infty d/\nu$
 SPL = Sound pressure level (dB)
 St = Strouhal Number based on excitation frequency
 T_i = Freestream turbulence intensity $= (u'^2)^{0.5}/U_\infty$
 U_∞ = Upstream velocity
 U_m = Streamwise mean velocity
 u = Streamwise velocity fluctuation
 v = Normal velocity fluctuation
 y = Radial distance measured from cylinder surface
 ν = Fluid kinematic viscosity
 θ = Angular position from geometric forward stagnation point

INTRODUCTION :

Controlling unsteady flow separation is of great importance in improving the performance of rotodynamic devices like helicopter rotor blades and axial compressor blades. The unsteady nature of separation in such devices is primarily characterized by the presence of a large-scale vortex-induced adverse pressure gradient. The flow inside the attached boundary layer often goes through a cycle of forward and reversed velocities before breaking away from the wall. When the attached flow separates over a lifting surface, a loss in lift usually follows. However, unlike flow over fixed lifting surfaces, the location of the separation point and resulting stall pattern in these cases are time dependent. Unsteady effects can be exploited to enhance lift since the onset of flow separation is delayed. However, when the flow ultimately separates, large unsteady aerodynamic forces and moments are generated. These

¹Research Assistant, Student Member AIAA

²Associate Professor, Senior Member AIAA

can lead to premature structural failure. Examples of undesirable unsteady flow separation induced effects include, dynamic stall on helicopter rotor blades and rotating stall on axial compressor blades.

The spatial location of the separation point and the exact instant in time when the attached boundary layer begins to break away are generally not available *a priori* for the above mentioned flows. Hence, a system for controlling unsteady separation can be expected to incorporate an array of individually controllable wall actuators and sensors in a feedback loop³. Nelson et al.⁴ recently implemented this strategy by using microphones as sensors and wall-suction as the actuator for controlling boundary layer transition on a flat plate. The control of laminar-turbulent transition or wall skin friction involves modifying the shape of the near-wall velocity profile. Therefore, devices or techniques used to delay transition or reduce skin friction can also be used to delay or promote separation. Several actuation mechanisms, ranging from oscillating flaps to jet vortex generators⁵, have been used to control flow separation. However, the mechanical complexity of these devices often make them impractical for use on moving components like compressor rotor blades.

One way of overcoming this problem is to use an array of active compliant wall actuators. With suitable material selection these actuators can be extremely simple and robust since they do not incorporate complicated mechanisms. Compliant passive walls of different stiffness and damping properties^{6,7} have been found to have varied effects on unstable waves on aerodynamic surfaces. By selecting the correct combination of these properties, along with the appropriate actuation parameters (i.e., forcing frequency, amplitude and wavelength of small-scale surface waves), it is possible to tailor the near wall velocity profile to achieve a desired objective. The objective may be drag reduction, transition delay or separation prevention. However, the correct combination of properties and actuation parameters has remained rather elusive. For example, an experimental study by Weinstein⁸ showed negligible drag reduction in a zero pressure gradient turbulent boundary layer when perturbed by an array of acoustically driven flexible wall membranes. Bushnell et al., in their review paper⁹ on drag reduction, commented on the effectiveness of modulating motions of passive compliant walls in drag reduction. The main problem identified by them was the unavailability of materials to construct walls having the requisite properties to deal with a large range of flow conditions.

An oscillating wall or membrane can also generate sound and interact with incident acoustic radiation. Experimental observations of Ahuja et al.^{10,11} suggested the possibility of using acoustic excitation for deterring turbulent boundary layer separation over airfoils. Other investigations have followed. Hsiao et al.¹² used a speaker-type internal acoustic source to study lift enhancement and drag reduction in

flows over circular cylinders and airfoils. Single-frequency sound wave from a speaker was used to emanate sound through a narrow slot on the surface. Separated boundary layers on cylinders and airfoils could be reattached at subcritical Reynolds numbers provided the sound pressure level (SPL) was high enough. Lower SPL was needed for internal excitation compared to external excitation by speakers mounted on the tunnel walls. Although, acoustic radiation was assumed to be responsible for controlling the separation, subsequent experimental investigations of Williams et al.¹³ suggest otherwise. An apparent lack of scaling with the SPL was observed, along with the fact that significant non-acoustic flow perturbation modes were generated by the acoustic sources used. This observation was later verified by the present authors¹⁴, who showed that flow separation control is possible only if the perturbation velocities, as measured by hot-film velocity probes, are fairly high. These perturbation velocities are several orders of magnitude higher than the particle velocities corresponding to the measured SPL values. As the flow Reynolds number increases, the effective perturbation frequencies also increase. The same acoustic speaker cannot produce large enough velocity perturbations at higher frequencies, thereby becoming ineffective.

An active compliant wall transducer can therefore be expected to interact with an attached boundary layer flow mechanically, with acoustic interactions playing a secondary role. The overall interaction will be a combination of flow-induced surface oscillations along with motions produced by internal driving. This paper investigates these interactions experimentally on a nominally two-dimensional oscillatory separating flow over a circular cylinder. An improved compliant wall transducer was constructed for this purpose. The results obtained are expected to provide a guideline for developing such transducers for flow separation control.

EXPERIMENTAL FACILITY :

A 155-mm diameter cylinder was placed in crossflow in a 600-mm x 600-mm test section of a subsonic wind-tunnel. The aspect ratio (l/d) and blockage ratio (H/d) were both 3.9. The flow Reynolds number (Re_d) was varied from 1.2×10^5 to 1.7×10^5 . The Strouhal number based on the vortex-shedding frequency remained practically constant at 0.21 at these Reynolds numbers¹². At two locations on the convex boundary, the oscillatory flow induces intermittent separation due to the adverse pressure gradient produced by the vortices shed from the cylinder¹. The compliant wall transducer array was mounted such that it spanned such a location (see next paragraph). The turbulence intensity (Ti) inside the test-section was less than 0.3% for the entire range of flow velocities (U_∞). The flow Mach number, based on boundary layer edge velocity (U_∞), was of the order of 0.07 to 0.13. Therefore, the flow over the entire

cylinder surface was considered to be incompressible (except for the effects of small-amplitude acoustic radiation). In order to study the effect of wall actuation on a fully turbulent boundary layer as well, provision was made for placing a sand-paper trip on the cylinder surface. The typical roughness height of the sand-paper was about 1-mm. Smoke-flow visualization was carried out for both un-tripped and tripped flow conditions to record the macro-scale movement of the unsteady separation point. A schematic of the experimental setup is shown in Figure 1(a).

The Transducer

An active compliant surface¹⁵ consisting of an array of thin strip-shaped conducting transducer elements, was flush mounted onto the upper surface of the cylinder (Figure 1(b)). Each strip had dimensions of 1.6 mm. in the streamwise direction and 500 mm. along the cylinder span. The strips were oriented parallel to the cylinder axis at an interval of 1 mm. in the streamwise direction. A compliant single-side aluminized Mylar membrane, with the aluminized side facing out, was used to cover the transducer elements. The edges of the membrane were glued onto the cylinder surface such that there was adequate tension in the membrane to avoid surface roughness. The entire compliant wall system covered the angular location of $\theta = 65^\circ - 100^\circ$ on the cylinder surface. The metallized Mylar film formed a capacitive motion transducer with each of the conducting strips. The stiffness (or compliance) of the wall could be controlled by varying the DC bias voltage between the metallized side of the mylar membrane and the conducting strips. In every case, a small air gap existed between the bottom of the Mylar and the conducting strips. Each strip in this configuration could be therefore be individually energized by a sinusoidal voltage signal to cause small-amplitude vibration of the wall.

Additionally, each strip in the above mentioned array was also designed to be used as a sensor for measuring flow fluctuation energy near the compliant wall. The output voltages from the sensing elements were proportional to changes in capacitance above each strip. As long as the surface Mylar sheet did not buckle due to skin friction, changes in capacitance are produced due to wall pressure fluctuations generated by the flow of air over the exposed surface of the transducer.

The maximum surface displacements of the transducer elements, when excited sinusoidally (at 20 volts amplitude for this study) were found to be very small (in the order of 10^{-3} -mm, as measured by a laser-Doppler vibrometer). This corresponded to a maximum normal surface velocity of about 15 mm/s. This was about three orders of magnitude lower compared to the freestream velocity. In contrast, bleed velocities at the slot of the acoustic speaker type exciter used by the authors in a previous

study¹⁴ needed to be around 8.0 m/s; comparable to the oncoming freestream velocities (e.g. 5-15 m/s) for effective control. Lower bleed velocities did not achieve the same degree of control with the speaker-slot device. The DC bias voltage on the compliant wall transducer was kept constant at 400 volts. This was seen to be sufficient for avoiding buckling of the membrane. Varying wall compliance did affect the frequency content of the sensed fluctuation signals. The energy consumed to vibrate the wall was found to be minimal (of the order of a few microwatts). This is also about four orders of magnitude lower compared to the speaker-slot device in earlier studies.

A single component hot-film probe (TSI Model 1210-60) was used to measure the mean and fluctuation velocities (U_m , u_{rms} and v_{rms}) at various points; close to the compliant wall, in the separated shear layer, and inside the attached boundary layer. A two component hot film probe (TSI Model 1241-20) was used to measure mean and fluctuation velocities inside the cylinder wake. Velocity profiles inside the attached boundary layer were also accurately measured using a boundary layer hot-film probe (TSI Model 1218-20). The hot film systems had an uncertainty of ± 6 cm/s (95% confidence level)¹⁶ for velocities in the range of 0.1 to 35 m/s.

Additionally, a differential pressure transducer (SETRA Model 264), communicating sequentially with surface mounted static-pressure taps, was used to detect changes in the mean (i.e. time-averaged) surface static pressures resulting from the compliant wall actuation. The time-averaged pressures had an uncertainty of ± 1.432 Pa in 75 Pa within a 95% confidence level¹⁶. The acoustic frequency response and the sound pressure level (SPL) of the wall vibration were measured with a 1/2 inch (12.5 mm) B & K condenser microphone. The SPL at the surface was maintained at 80 dB above the ambient noise level. Even though acoustic effects may not account for interaction with the flow, measuring the SPL provides a direct measure of surface oscillation amplitudes with a narrow frequency range. Lower SPL values were found to be considerably less effective in separation control. The acoustic frequency responses of three representative transducer elements (in the streamwise direction) are shown in Figure 2. The variation in acoustic response along the length (i.e. along the cylinder span) of each strip was within 7%.

RESULTS AND DISCUSSIONS :

The micro-scale motion of the active compliant wall was found to be beneficial in delaying unsteady separation over the circular cylinder for the Reynolds number range considered in this study. The transducer strips were designed so as to introduce nominally two-dimensional streamwise disturbances. For the frequencies used in this study, the acoustic wavelengths

were significantly larger than the streamwise width of the strips. Hence the strips have been assumed to behave as line sources. The exact interaction mechanisms between the wall perturbation and the near-separation boundary layer flow is complex. However, some interesting changes in the flowfield variables could be measured with consistent accuracy and repeatability so as to permit a qualitative study of the separation point movement.

The optimum Strouhal number (St_s) for controlling the separating boundary layer flow with the active compliant wall was found to be about 23. This is an order of magnitude higher than those reported with external and internal acoustic excitations^{10,11,12}, thereby suggesting a different flow-perturbation interaction mechanism. The strips were excited one at a time, and changes in mean surface static pressures were noted. Once the optimum angular location (θ) for the point of excitation was determined, the effect of driving multiple elements (in phase) was determined. For $Re_d = 1.5 \times 10^5$, largest changes in mean static pressures were observed when two adjacent strips, spanning the region between $\theta = 72^\circ$ - 74° from the mean forward stagnation point, were excited at 2.25 kHz. The selection of the excitation frequency (f_s) at this Re_d was based on the information obtained from one of the transducer element acting as a wall pressure fluctuation sensor. Figures 3 shows the spectrum of wall pressure fluctuation downstream ($\theta = 78^\circ$) of the excitation point at this Re_d , in absence of any excitation. The pressure spectrum near the time-averaged mean separation point² shows a peak at 2.25 kHz. It is important to note that the transducers did not have any mechanical or acoustic resonances at this frequency. Therefore, this frequency indicates a flow-induced instability near the separation point.

Changes in mean lift and drag :

Figure 4 shows the changes in mean surface pressures as a result of exciting two actuator elements in unison between 72° and 74° . A mean coefficient of lift (C_L) of 0.15 was observed when no acoustic excitation was used. The mean C_L on a rigid circular cylinder should have been zero. The presence of the compliant wall on one side, though mounted nearly flush on the cylinder upper surface ($\theta = 65^\circ$ - 100°), changed the mean pressure distribution on the cylinder. This change (i.e. under unexcited conditions) can be attributed to the additional compliance, damping or roughness introduced by the passive wall. When wall actuation was used to perturb the flow ($f_s = 2.25$ kHz, at $\theta = 72^\circ$ - 74°), the mean lift coefficient, C_L , increased to 0.47. A corresponding decrease in form drag of 12.4% was also noted. Lift and drag forces were estimated by numerical integration of the time-averaged static pressure distribution data over the entire cylinder.

Changes in velocity fluctuation spectra :

Single component hot-film measurements close to the cylinder surface, both upstream and downstream of the optimum excitation region, showed an increase in the time-averaged streamwise mean velocities (U_m) when the actuator elements were energized. The corresponding fluctuation component of velocity decreased (Figures 5(a) and 5(b)). Figure 5(a) shows the time-averaged spectra of resultant velocity fluctuations in the unexcited and excited boundary layers, at $\theta = 74^\circ$ from forward stagnation (i.e. pre-separation, even under unexcited conditions). Figure 5(b) shows the same but at a location where the unexcited boundary layer has already separated ($\theta = 82^\circ$). It is interesting to note that no peaks corresponding to the excitation frequency (2.25-kHz) appear in these figures.

Figure 6 shows the distribution of mean and fluctuation velocities close to the surface ($y = 1$ mm for all measuring stations) for the flow at $Re_d = 1.5 \times 10^5$ and clearly shows the delay of separation brought about by wall actuation. The time-averaged separation point was close to $\theta = 78^\circ$ and, under acoustic excitation, moved downstream to $\theta = 106^\circ$ from forward stagnation point. Maximum velocity fluctuations decreased as a result of excitation and also the location of maximum flow fluctuations receded back to $\theta = 106^\circ$ from $\theta = 80^\circ$ as a result of delayed separation.

Two-component velocity measurements were performed inside the wake region using the two-component hot-film probe. This assumes that the spanwise components of velocities (w) are significantly smaller than the other two components (u and v). Measurements showed that both streamwise and normal components of velocity increase as a result of forcing. Figures 7(a) and 7(b) show the distributions of mean and fluctuation velocities inside the cylinder wake. The normalised wake height ($2h/d$) is defined as the ratio of the vertical distance (measured from the horizontal midplane of the cylinder) to the cylinder radius. Under wall excitation ($f_s = 2.25$ kHz and $\theta = 72^\circ$ - 74°), both the mean velocity components increased remarkably, whereas the velocity fluctuations decreased. It suggests that the size of the wake region diminished and the flow unsteadiness due to vortex-shedding was reduced under excitation. The large asymmetry in mean velocities at the top and bottom half of the wake is due to the asymmetric location of the compliant wall. Recently experiments were repeated with a second compliant wall located on the lower surface of the cylinder. While the flow symmetry was partially restored as a result of this some differences remained. These are currently being investigated. Differences in transducer properties and bias errors in the velocity measurements are believed to be the principal causes.

Since the flow Reynolds number, at which the effect of compliant wall perturbation was studied, was very close to the transitional Reynolds number for the cylinder, it was

apprehended that the forcing actually facilitates the laminar-turbulent transition process. To study the effect on a fully turbulent boundary layer, the flow over the cylinder was tripped at $\theta = 35^\circ$ using a sand-paper trip. To ensure that the flow had actually become turbulent, single-element hot-film probe measurements were carried out very close to the cylinder upper surface. The optimum point of excitation for the tripped boundary layer was again found to be $\theta = 72^\circ$ - 74° . A significant change in mean static pressure distribution was observed due to wall actuation (Figure 8). The nature of static pressure change in this case was different than that obtained by exciting the undisturbed (or, untripped) boundary layer. Excitation of the tripped boundary layer produced an overall change in the surface pressure distribution in the cylinder wake ($\theta = 95^\circ$ to $\theta = 300^\circ$). Numerical integration of the pressure distributions under two different conditions (unexcited and acoustically excited) indicated that the average lift coefficient (C_L) changed from 0.33 to 0.54 under excitation. Also, the pressure-drag force was reduced by 20.2% due to the change in surface pressure distribution in the wake region.

Flow Visualization :

Smoke flow visualizations of both the untripped and tripped flow situations showed that separation could be delayed by wall excitation on the cylinder upper surface. The near-separation unsteadiness of the untripped flow could also be reduced considerably (a video of the flow visualization experiments available with the authors clearly shows this). Figures 10(a) and 10(b) show the smoke line pattern on the upper surface of the cylinder under unexcited and excited state. The flow was untripped in both the pictures. Figures 11(a) and 11(b) show the same for the tripped flow condition. It can be observed that the achieved extent of separation control is more in case of an untripped flow. Another observation was that the separated shear layer could be made to reattach almost instantaneously by commencing the excitation. The flows reverted back to their original states upon removal of the excitation. For Reynolds numbers lower than about 1.2×10^5 , the reattachment was seen to be intermittent. Below 1.0×10^5 no changes could be visualized.

CONCLUSIONS AND RECOMMENDATIONS :

In this experimental study, an attempt has been made to characterize the interaction of a separating flow with an active compliant wall. Experimental observations lead to the conclusion that compliant wall actuation can be successfully used to delay unsteady flow separation over convex boundaries within a range of flow Reynolds numbers. The range of Reynolds numbers and flow configurations amenable to this form of control remains to be explored. Additional experiments performed by the present authors (to be reported elsewhere)

have shown that this control also works on controlling flow separation on airfoils.

For the present experiments no changes were observed when the SPL, resulting out of the high frequency vibration of the compliant wall, was less than 70 dB. Also, significantly higher SPL values (e.g. 100 dB) did not produce noticeable improvement. If the disturbances are introduced further upstream, they get attenuated by the flow to levels comparable to the turbulent fluctuations, and are therefore ineffective. The acoustic wavelength in air at the optimum excitation frequency of 2.25 kHz is about 145-mm. This was not close to any of the known resonant modes in the wind-tunnel. Furthermore, this wavelength was significantly larger than the maximum boundary layer thickness (about 2-mm). Hence the acoustic component of the disturbances perturbed the freestream flow as well (i.e. similar to external acoustic excitation). Tam¹⁷ discussed the possibility of triggering unstable Tollmien-Schlichting (TS) waves in a shear layer as a result of incident acoustic waves. A similar possibility may exist in this case because the instantaneous velocity field in the near separation attached boundary layer on a cylinder has a sharp gradient.

The compliant wall vibration reduced the resultant velocity fluctuations near the wall. This reduction at practically all frequencies can be attributed to a flow of velocity-fluctuation energy towards pressure-fluctuation energy. When the flow is excited, pressure fluctuations are found to increase at the excitation frequency. However, it is still a speculation, which needs to be verified. Additionally, the changes in mean static pressure on the surface of the cylinder indicated lift enhancement and drag reduction. Since large-scale velocity and pressure fluctuations due to vortex-shedding are superposed on small-scale instabilities, the phase relation of the two is of great significance. The pressure fluctuations sensed by the individual strips contain a wide range of frequencies, and further signal processing will be required in order to track the separation point more accurately. The wall excitation suggests that a phased oscillation of a number of actuating elements may successfully control the size of a selected vortical structure. At the same instance, it is also important to select a proper location of excitation such that the relatively small-strength perturbation can grow nonlinearly inside the attached boundary layer and can modify the naturally occurring flow disturbances. Issues related to flow asymmetry are currently being investigated. The results of these studies are expected to reveal additional information regarding the effects of transducer properties on the range and efficacy of this form of control.

ACKNOWLEDGEMENT S:

This research was initiated through support through a

grant (No. AFOSR 91-0410) from the Air Force Office of Scientific Research, under the mentorship of Major Daniel Fant. The continuation work has been partially funded by Grant No. DAAH-04-93-G-0451 from the Army Research Office under the Mentorship of Dr. Thomas Doligalski. The authors gratefully acknowledge this support.

REFERENCES :

- ¹Farrel, C., and Blessman, J., "On Critical Flow around Smooth Circular Cylinders", *Journal of Fluid Mechanics*, Vol. 136, 1983, pp. 375-391.
- ²Schlichting, H., "Boundary Layer Theory", McGraw Hill, 1968
- ³Sinha, S.K., and Shields, F.D., "Acoustically Active Surfaces for Boundary Layer Control," ASME Winter Annual Meeting, Atlanta, GA, December 1991, PVP-Vol.224/FED Vol.126, pp. 17-19.
- ⁴Nelson, P.A., Rioual, J.L., and Fisher, M.J., "Experiments on the Active Control of Transitional Boundary Layers," *Proceedings of the Second International Congress on Recent Developments in Air and Structure Borne Sound and Vibration*, Auburn University, March 1992, pp. 305-312.
- ⁵Gad-el-Hak, M., and Bushnell, D.M., "Separation Control: Review", *ASME Journal of Fluids Engineering*, Vol. 13, 1991, pp. 5-30.
- ⁶Carpenter, P.W., and Garrad, A.D., "The Hydrodynamic Stability of Flow over Kramer type Compliant Surfaces. Part 1. Tollmien-Schlichting Instabilities", *Journal of Fluid Mechanics*, Vol. 155, 1985, pp. 465-510.
- ⁷Carpenter, P.W., and Garrad, A.D., "The Hydrodynamic Stability of Flow over Kramer type Compliant Surfaces. Part 2. Flow-Induced Surface Instabilities", *Journal of Fluid Mechanics*, Vol. 170, 1986, pp. 199-232.
- ⁸Weinstein, L.M., "Effect of Driven Wall Motion on a Turbulent Boundary Layer", *IUTAM Symposium on "Unsteady Turbulent Shear Flows"*, Toulouse, France, 1981.
- ⁹Bushnell, D.M., Hefner, J.N., and Ash, R.L., "Effect of Compliant Wall Motion on Turbulent Boundary Layers", *Physics of Fluids*, Vol. 120, No. 10, Part II, October, 1977.
- ¹⁰Ahuja, K.K., Whipkey, R.R., and Jones, G.S., "Control of Turbulent Boundary Layer Flows by Sound", *AIAA 8th Aeroacoustics Conference*, April 1983, Atlanta, Georgia, AIAA-83-0726.
- ¹¹Ahuja, K.K., and Burrin, R.H., "Control of Flow Separation by Sound", *AIAA/NASA 9th Aeroacoustics Conference*, October 1984, Williamsburg, Virginia, AIAA-84-2298.
- ¹²Hsiao, F.B., Liu, C.F., and Shyu, J.Y., "Control of Wall Separated Flow by Internal Acoustic Excitation", *AIAA Journal*, Vol.28, No.8, 1990, pp.1440-1446.
- ¹³Williams, D., Acharya, M., Bernhardt, J., and Yang, P., "The Mechanism of Flow Control on a Cylinder with the Unsteady Bleed Technique", *AIAA Paper No. 91-0039*.
- ¹⁴Sinha, S., and Pal, D., "On the Differences between the Effect of Acoustic Perturbation and Unsteady Bleed in Controlling Flow Separation over a Cylinder", *SAE Aerotech '93*, California, September 1993, Paper No. 932573.
- ¹⁵Sinha, S.K., "The ACOUSTOSURF - a Multi-Element Acoustic Active Surface for Flow Separation Control", Patent pending.
- ¹⁶Coleman, H.W., and Steele, W.G., "Experimentation and Uncertainty Analysis for Engineers", John Wiley and Sons, 1989.
- ¹⁷Tam, C.K.W., "Excitation of Instability Waves in a Two-dimensional Shear Layer by Sound", *Journal of Fluid Mechanics*, Vol. 89, Part 2, 1978, pp. 357-371.

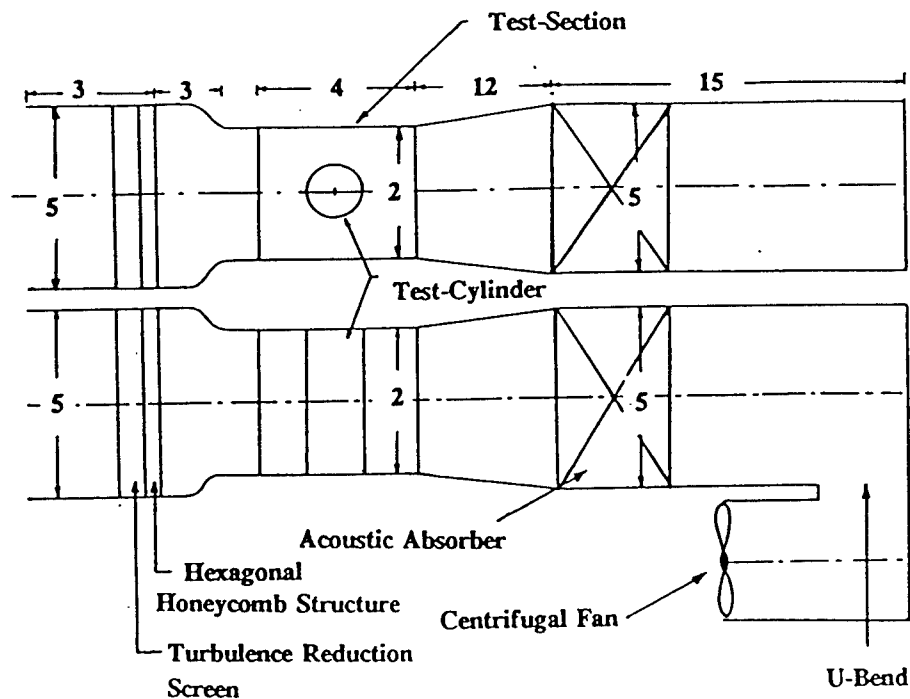


Figure 1 (a). Wind-tunnel testing facility . All dimensions in ft.

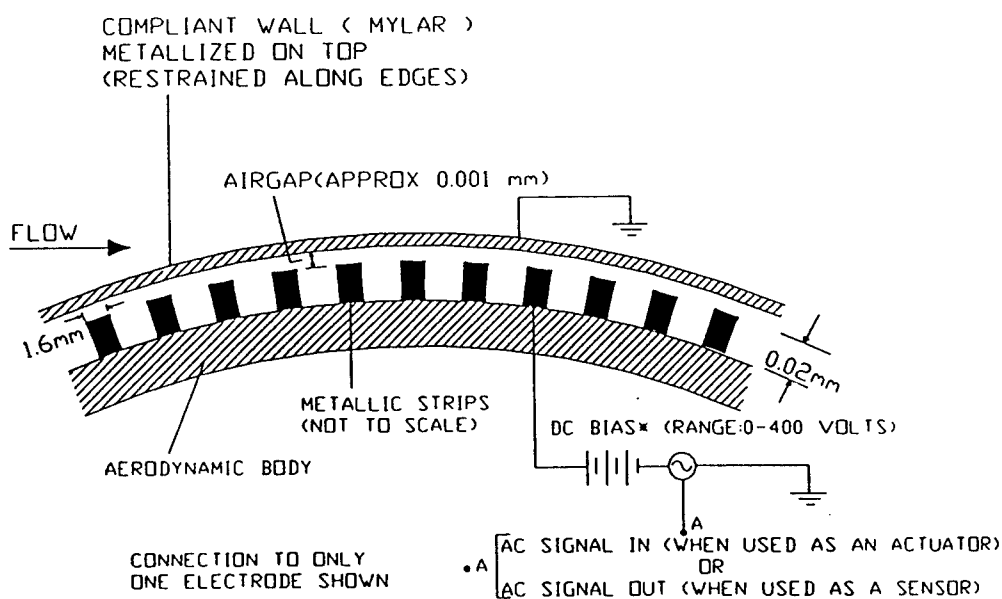


Figure 1 (b). Construction details of the array of compliant wall elements. Wall compliance depends on the D.C. bias voltage.

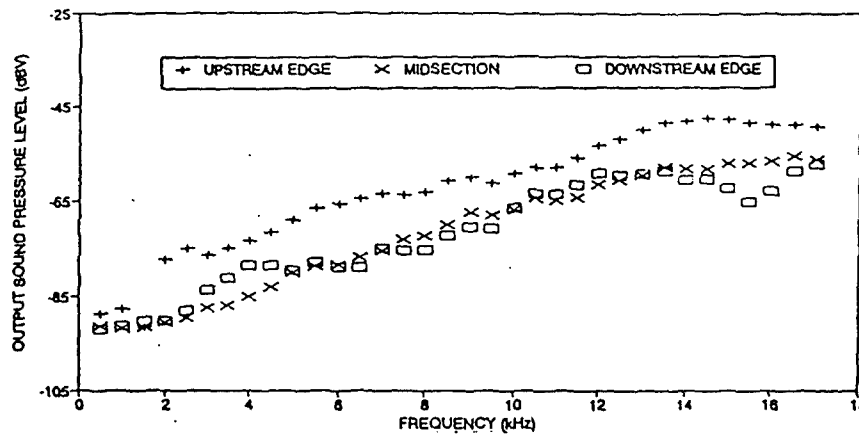


Figure 2. Acoustic frequency response of three different compliant wall elements. (upstream edge, midsection and downstream edge).

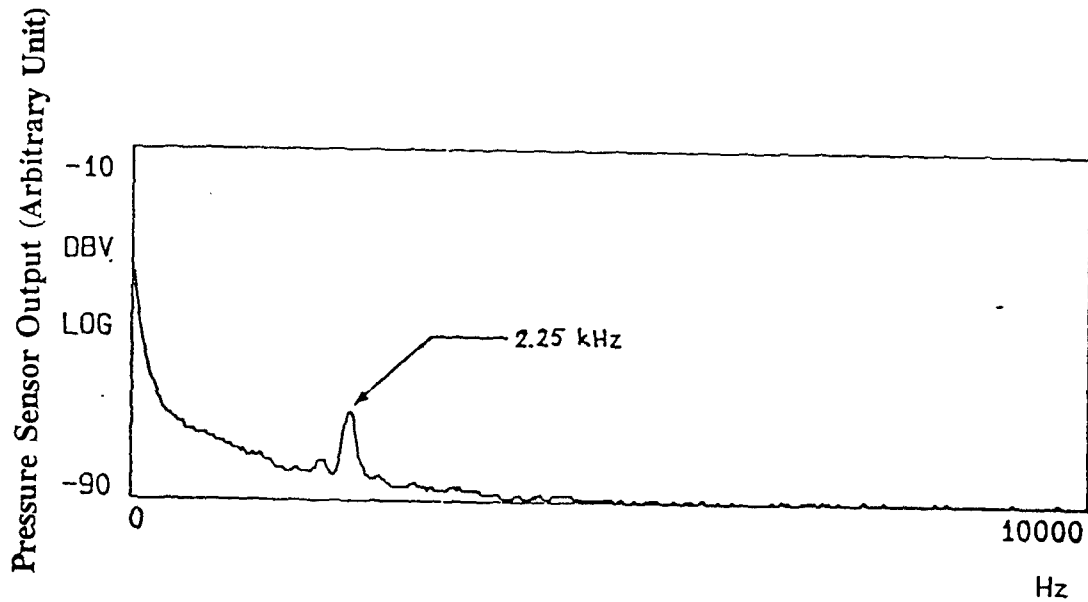


Figure 3. Time-averaged surface pressure spectrum of pre-separation boundary layer in the absence of compliant wall actuation. $Re_d = 1.5 \times 10^5$. Measurement location : $\theta = 78^\circ$.

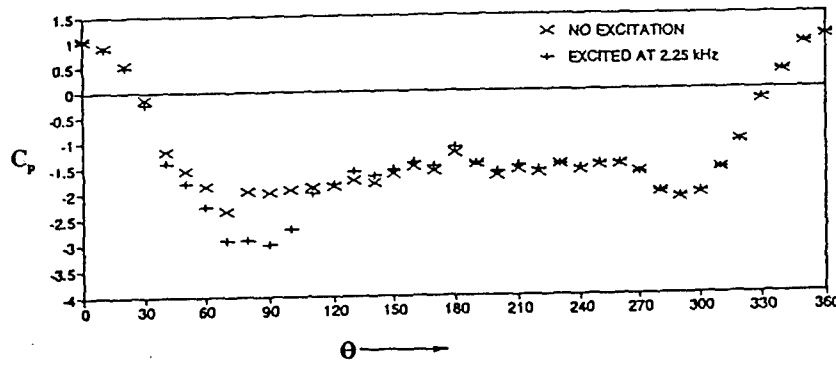


Figure 4. Surface static pressure distribution (unexcited and excited flow states). $Re_d = 1.5 \times 10^5$. $f_s = 2.25$ kHz. Location of excitation : $\theta = 72^\circ - 74^\circ$ (multiple strip excitation).

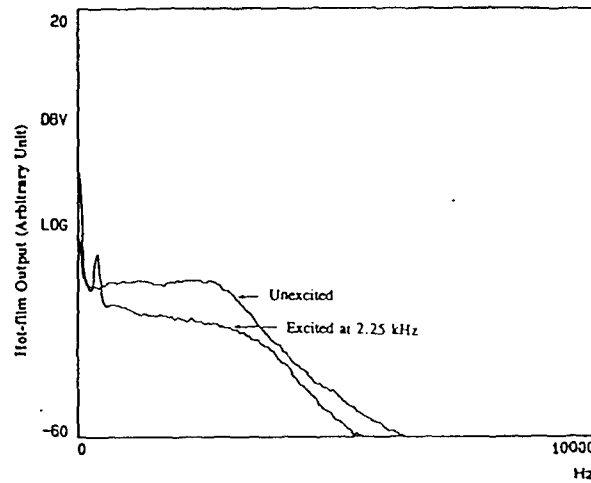


Figure 5 (a). Time-averaged velocity spectra of pre-separation boundary layer . $Re_d = 1.5 \times 10^5$. $f_s = 2.25$ kHz. Location of excitation : $\theta = 72^\circ - 74^\circ$ (multiple strip excitation). Measurement location : $\theta = 74^\circ$, $y = 2$ mm.

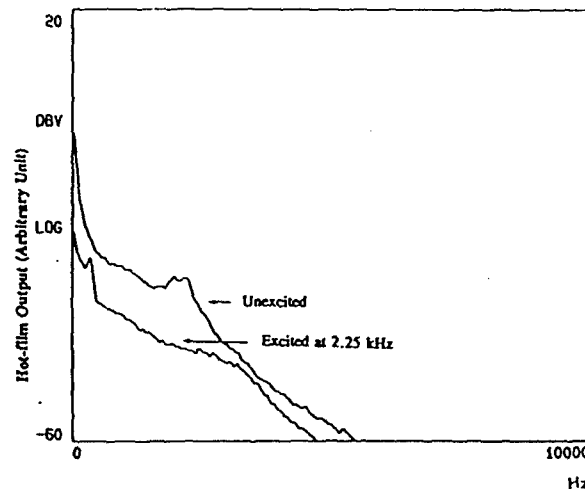


Figure 5 (b). Time-averaged velocity spectra of post-separation shear layer. $Re_d = 1.5 \times 10^5$. $f_s = 2.25$ kHz. Location of excitation : $\theta = 72^\circ - 74^\circ$ (multiple strip excitation). Measurement location : $\theta = 82^\circ$, $y = 8$ mm.

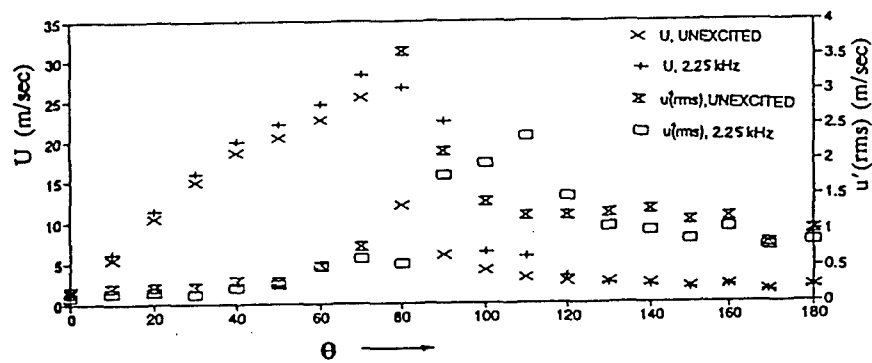


Figure 6. Distribution of time-averaged mean and fluctuation velocities close to the cylinder surface. $y = 1$ mm for all measurement locations. $Re_d = 1.5 \times 10^5$. $f_a = 2.25$ kHz. Location of excitation : $\theta = 72^\circ - 74^\circ$ (multiple strip excitation).

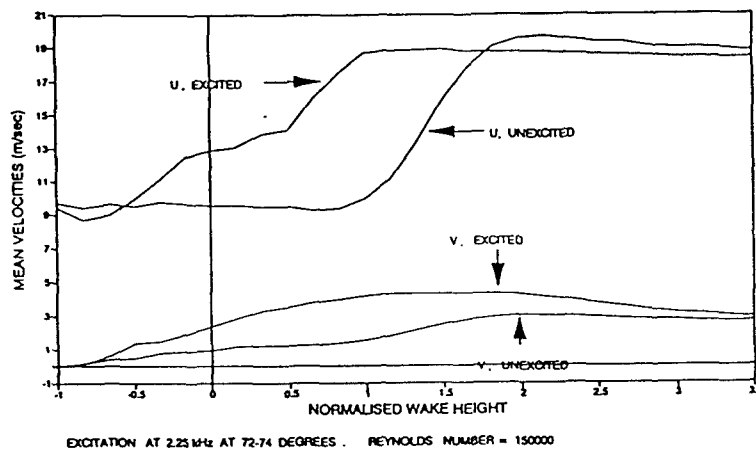


Figure 7 (a). Distribution of streamwise and normal component of mean velocity in the cylinder wake. Measurement location : $1.5d$ from the cylinder center.

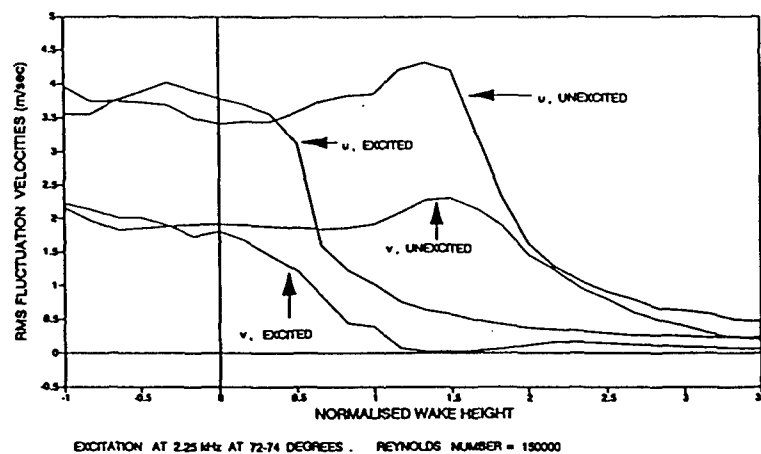


Figure 7 (b). Distribution of streamwise and normal component of velocity fluctuations (rms) in the cylinder wake. Measurement location : $1.5d$ from the cylinder center.

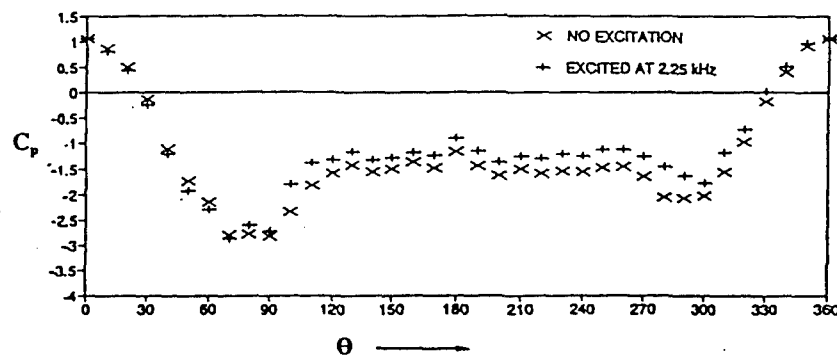


Figure 8. Surface static pressure distribution (unexcited and excited flow states). $Re_d = 1.5 \times 10^5$. $f_s = 2.25$ kHz. Artificial flow tripping at $\theta = 35^\circ$. Location of excitation : $\theta = 72^\circ - 74^\circ$ (multiple strip excitation).

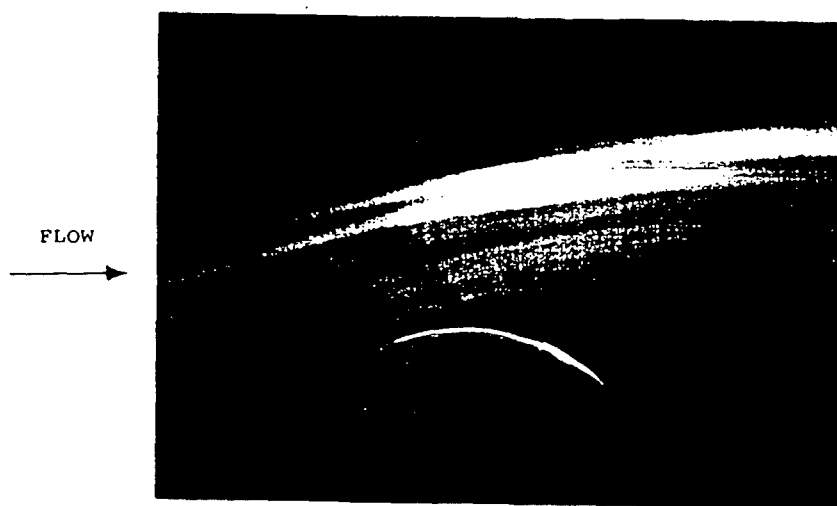


Figure 9 (a). Smoke flow visualization of the untripped flow in absence of the wall actuation. $Re_d = 1.5 \times 10^5$.

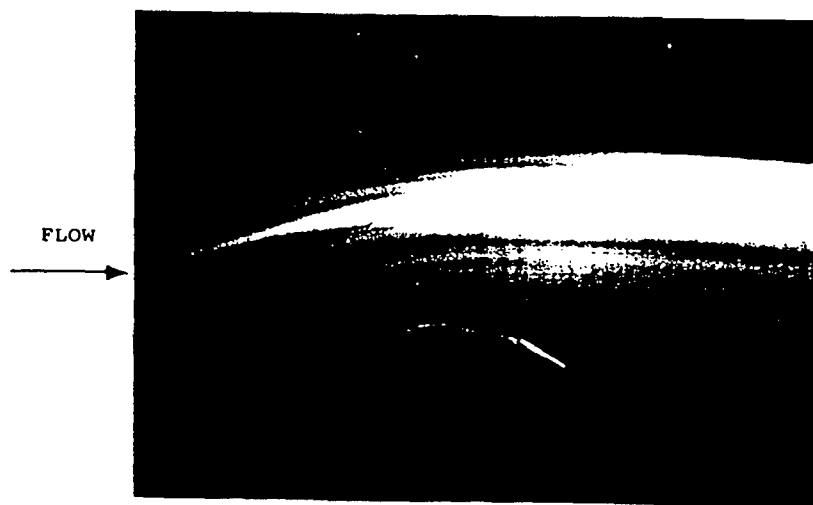


Figure 9 (b). Smoke flow visualization of the untripped flow with wall actuation at $\theta = 72^\circ - 74^\circ$. $f_s = 2.25$ kHz. $Re_d = 1.5 \times 10^5$.



Figure 10 (a). Smoke flow visualization of the tripped flow in absence of the wall actuation. $Re_d = 1.5 \times 10^5$. Artificial flow tripping at $\theta = 35^\circ$.

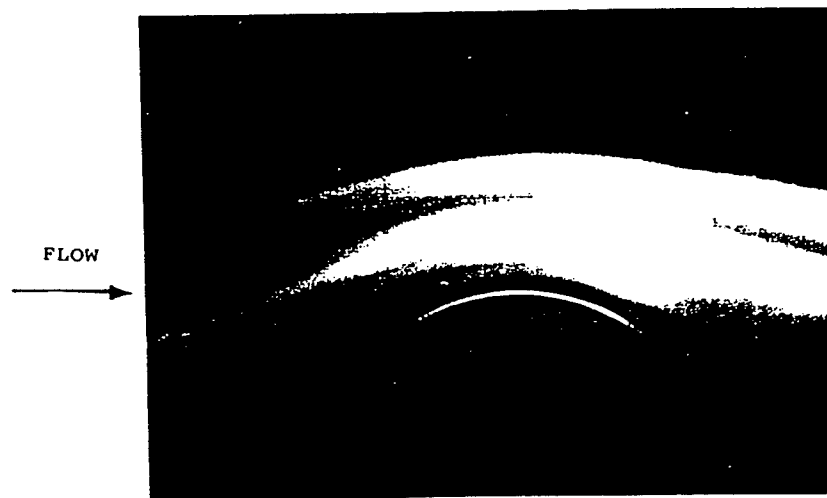


Figure 10 (b). Smoke flow visualization of the tripped flow with wall actuation at $\theta = 72^\circ$ - 74° . $f_a = 2.25$ kHz. $Re_d = 1.5 \times 10^5$. Artificial flow tripping at $\theta = 35^\circ$.

ABSTRACT

AN EXPERIMENTAL INVESTIGATION OF FLOW SEPARATION CONTROL USING AN ACOUSTIC ACTIVE SURFACE

BANERJEE, DEBJYOTI

B. Tech. (Honours), Indian Institute of Technology (Kharagpur), 1992.

M.S., The University of Mississippi, 1995.

Thesis directed by Dr. Sumon K. Sinha.

The phenomenon of flow separation is usually detrimental towards the performance of fluid mechanical devices. Various methods have been used to control flow separation in practical applications. However, a need exists for devices with better efficacy (e.g., less mechanical complexity) and a broader range of effective operational regimes. In this respect active devices offer an advantage over passive methods.

Recent developments show that effective separation control can be achieved by means of active devices using acoustic sources, like acoustic speakers. Though acoustic speakers were found to be effective in controlling flow separation in low Reynolds

number laboratory studies, high energy requirements in real (high Reynolds number) applications have limited their practical use. Of recent interest has been the development of an acoustic transducer ("acoustic active surface"), which consists of an array of narrow strip shaped sources of acoustic radiation. This transducer has been shown to be highly efficient in controlling unsteady flow separation over a cylinder. The control action was achieved by expending energy that is orders of magnitude smaller compared to conventional methods. In the present work, flow visualization studies revealed the process of separated flow reattachment over a cylinder achieved by activation and deactivation of the acoustic active surface. Subsequently, flow visualization along with velocity and surface pressure measurements were used to establish the feasibility of using the acoustic active surface in controlling flow separation over a NACA-0012 airfoil at fairly high (transitional to turbulent) chord based Reynolds numbers (4.3×10^5 and 8.25×10^5). Results of these experiments confirm that the surface interacts with the flow through flow-acoustic interactions along with the surface compliance effects. The results show the existence of a different scaling law at higher Reynolds numbers. The acoustic active surface was found to be most effective in controlling transitional and turbulent leading edge flow separation at near separation angles of attack of the airfoil. Compared to flow over a cylinder, the process of separation control for flow over an airfoil is found to be significantly different. The control action is slightly delayed. Also the flow does not re-separate upon de-activation of the surface.